Hindawi
International Journal of Polymer Science
Volume 2019, Article ID 3403548, 23 pages
https://doi.org/10.1155/2019/3403548

Review Article

Polymers for Regenerative Medicine Structures Made via Multiphoton 3D Lithography

Greta Merkininkaitė,[1,2] Darius Gailevičius,[1,3] Simas Šakirzanovas,[2] and Linas Jonušauskas[1,3]

[1]*Femtika, Sauletekio Ave. 15, Vilnius LT-10224, Lithuania*
[2]*Faculty of Chemistry and Geoscience, Vilnius University, Naugarduko Str. 24, Vilnius LT-03225, Lithuania*
[3]*Laser Research Center, Physics Faculty, Vilnius University, Sauletekio Ave. 10, Vilnius LT-10223, Lithuania*

Correspondence should be addressed to Linas Jonušauskas; linas@femtika.lt

Received 2 August 2019; Accepted 5 October 2019; Published 3 December 2019

Guest Editor: Parisa P. Abadi

Multiphoton 3D lithography is becoming a tool of choice in a wide variety of fields. Regenerative medicine is one of them. Its true 3D structuring capabilities beyond diffraction can be exploited to produce structures with diverse functionality. Furthermore, these objects can be produced from unique materials allowing expanded performance. Here, we review current trends in this research area. We pay particular attention to the interplay between the technology and materials used. Thus, we extensively discuss undergoing light-matter interactions and peculiarities of setups needed to induce it. Then, we continue with the most popular resins, photoinitiators, and general material functionalization, with emphasis on their potential usage in regenerative medicine. Furthermore, we provide extensive discussion of current advances in the field as well as prospects showing how the correct choice of the polymer can play a vital role in the structure's functionality. Overall, this review highlights the interplay between the structure's architecture and material choice when trying to achieve the maximum result in the field of regenerative medicine.

1. Introduction

Additive manufacturing-based 3D printing is a revolutionizing field of technology which is gaining a substantial foothold in industry [1]. It offers new possibilities in producing various structures or entire devices in a relatively short time, minimizing the time from the idea to the final physical object. There are numerous different ways to realize the additive manufacturing method [1]; however, multiphoton polymerization-based 3D laser lithography (3DLL) stands out among all other current 3D printing techniques. The idea behind this technology is to sharply focus a laser (in most cases, femtosecond (fs)) beam into a special photoactive material initiating highly localized photomodification *via* multiphoton absorption and/or other related nonlinear light-matter interactions [2]. It combines resolution below the diffraction limit [3, 4], virtually no limitations to the 3D architecture of an object with the structuring process not bound to layer-by-layer printing [5, 6], and a huge variety of the materials that could be used [7, 8]. Due to this, it was used in numerous fields, which include photonics [9, 10], microoptics [11, 12], micromechanics [13, 14], microfluidics [5, 15], and biomedicine [16, 17].

One of the key attributes in this technology is the vast array of suitable materials [7, 8]. Indeed, the requirements for the materials applicable to 3DLL are rather minimal: they have to be transparent to the laser wavelength and must possess absorption characteristics suitable for multiphoton absorption, which leads to photopolymerization. For this reason, materials such as acrylates [18], epoxies [19], hydrogels [20], hybrids [21], or biopolymers [22] were structured through the years using 3DLL. The correct choice of the material sometimes can be a main issue in a specific application. Thus, when talking about 3DLL and multiphoton polymerization, polymers and their properties should be one of the key aspects which needs to be addressed.

Among other 3DLL applications, regenerative medicine (RM) stands out as one with the most promise and possible

implications for everyday life. RM can be defined as the field which aims to replace, engineer, or regenerate human cells, tissues, or organs to restore or establish their normal functions [23]. However, the combination of achievable resolution, freedom of design, and applicable materials made RM one of the key research areas where 3DLL produced structures are being tested [24–26]. It enables to create objects that could help heal damaged tissue or even replace entire segments of the body. Besides the impressive possibilities, a lot more consideration has to be made in choosing both the geometry of the structure and the suitable polymer. The latter, alongside the two requirements mentioned previously, also have to be biocompatible and/or have properties beneficial for RM. Furthermore, RM research relies on structures with sizes well into the mm scale [16, 27, 28] and statistical testing based on simultaneous examination of multiple structures. This requires high-throughput fabrication. Thus, in RM applications, deep understanding of 3DLL technology and polymers is mandatory.

The main goal of this review is to explore 3DLL structurable polymers in the light of RM application. In order to present the reader with all the necessary information, we start by briefly introducing the basics of 3DLL technology. This includes both a brief discussion of underlying physical phenomena and the engineering required to realize it practically. Then, we proceed to 3DLL materials. Here, we discuss the main categories of polymers used in 3DLL. Photoinitiators (PIs) are also discussed in some detail because the correct choice of substance can lead to some very desirable (for instance, high throughput) or adverse (toxicity) effects. Additionally, the possibilities of polymer functionalization will follow. After that, various biomedical applications are shown with main attention on how in each case the correctly chosen material benefits it. Finally, we conclude by providing an outlook for the perspectives in the field, highlighting some of the challenges and opportunities currently present in this area. Relevant connections to other fields or structuring techniques are presented through the text to reference the usage of 3DLL in RM in the broader, more complete way. Finally, while this review is dedicated to RM, 3DLL was used with huge success in other biology and medicine-related fields, such as microfluidics [29] and in fabricating microneedles [30]. In order to avoid confusion, these areas will not be discussed in detail and only referenced in the context relevant to RM.

2. Multiphoton 3D Lithography

We will begin the review by discussing the fundamentals of 3DLL. These include mechanisms of multiphoton excitation, the kinetics of polymerization reaction, and which practical setups are required to realize it.

2.1. Multiphoton Excitation. In standard UV and stereolithography, the polymerization reaction is induced *via* linear one-photon absorption (Figure 1(a)) and the structure is formed layer by layer [1]. In that case, the photon energy E_p is equal or greater than the bandgap of the material E_g.

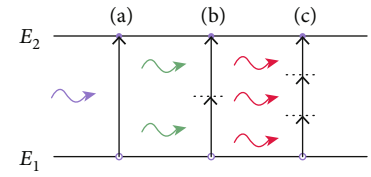

Figure 1: Energy level diagrams of one- (a), two- (b), and three- (c) photon absorption. Solid lines represent real arbitrary energy levels E_1 and E_2; dotted lines represent virtual states.

Keeping in mind that $E_p = h\nu = hc/\lambda$, it means that a shorter wavelength (λ) is needed. Here, we also introduced ν—the frequency of laser light. In most cases, UV light sources with $\lambda < 350$ nm are used. The absorption of the photon causes the electron to be exited from an energy state corresponding to the valence band to a state in the conduction band. This might lead to a multitude of outcomes. For instance, an electron might return to the valence band while heating up the material or emitting another photon causing fluorescence. However, it can also alter the chemical bond inducing chemical reaction. In the case of lithography, it is the polymerization reaction that cross-links the material. The exact pathways of such reactions will be discussed later. Light is a potent tool to induce such reactions because it can be done on-demand in localized regions. It is also a contactless method, meaning that there is no contamination to the sample or material by the processing tool.

One photon absorption has some distinct disadvantages. While collimated light can induce polymerization reaction in the relatively big (up to cm) area with high repeatably [31], achieving true 3D shapes is tricky. The standard way used in stereolithography is stacking 2D layers on top of each other. This leads to the necessity to use supports if free-hanging features are made [32]. Another way is using tilted/rotated samples [33]. Then, more geometries become available, yet it is still limited and rather complex process. Also, resins need to be liquid in order to cast a new layer after the previous one is done. Furthermore, if biomaterials are used, UV light might induce damage to the mixed-in living organisms. Therefore, direct bioprinting potential is limited. Finally, due to the nature of such polymerization, relatively significant amounts of unpolymerized resin might remain in the structure. As such resins are very chemically active, they might make manufactured structures toxic [34]. Thus, while one-photon absorption is a powerful tool for manufacturing various structures, including medical ones, there are also some severe limitations.

Linear absorption can be induced even with the low power noncoherent light sources. However, if the light intensity is increased, nonlinear absorption can take place. While such interaction was predicted as early as 1931 [35], it took the creation of the laser to demonstrate nonlinear absorption and subsequent fluorescence [36] experimentally. The absorption during this interaction is induced by the absorption of two or more photons *via* virtual levels (Figure 1(b)). Due to the extremely short lifetime of the virtual levels (~fs [37]), photons have to be absorbed almost simultaneously.

This leads to two important conclusions. First, such interaction is possible only with light intensities that are high enough (>GW/cm^2). Second, the probability of multiphoton interaction increases with the decrease in the number of photons involved in the single absorption event. Thus, the two-photon absorption (TPA) can be considered as the most likely process. This is well reflected in the fact that sometimes 3D manufacturing technology discussed in this article is called two-photon polymerization (2PP/TPP). For the sake of simplicity in this article, we will consider only this effect unless otherwise specified.

In TPA case, the number of photons absorbed n_p per time t can be calculated using the following equation:

$$\frac{dn_p}{dt} = \sigma_2 N F^2. \quad (1)$$

Here, σ_2 is the TPA cross-section of a particular material (quantified by Göppert-Mayer units, GM = 50^{-50} cm^4 s), N is the density of the absorbing component, and F is the photon flux which can be defined as $F = I/h\nu$. From Equation (1), we can draw conclusions about what practical considerations should be made when trying to apply TPA for polymerization. First, the photon absorption rate is proportional to I^2, making excessive I one of the main considerations. The N should also be sufficient for the reaction. Finally, the material needs to be reactive enough to have high σ_2. The first requirement is realized using an appropriate processing setup, the second and third by tuning the material properties. The nonlinearity of the process behind 3DLL is the key to achieving fabricated features below the diffraction limit as the threshold I might be well below the size of the laser spot. Due to it, sub-100 nm lines were directly structured using 3DLL [3, 4].

For the final note, it is important to stress that TPA is only one of many light-matter interaction regimes that might appear when matter is exposed to high I. Higher-order absorption can take place [38, 39]. Also, if the pulse duration is long enough, one can expect avalanche ionization to become comparable or even surpass TPA in chemical bond cleavage [2, 40]. Finally, in some cases, thermal effects can start to have an impact on the reaction [41, 42]. Keeping in mind all of this and the fact that there is an active discussion in the field about the nature and impact of some of these processes, one must be careful when naming discussed technology simply as 2PP/TPP. Using multiphoton 3D lithography or just 3DLL terms are a lot more general and correct options. This is especially true if exotic materials or nonstandard laser sources are used.

2.2. Polymerization Mechanisms. Knowing the principles that are important for understanding photoexcitation, we can now proceed to the photopolymerization process itself. The main goal of using light in lithography is to induce photocleavage of the chemical bond and initiation of photochemical reactions. As mentioned before, this is done by the multiphoton process in 3DLL. Depending on the peculiarities of the material, it produces radicals or cations. In turn, polymerization reactions can be divided into radical and cationic polymerization [43]. Schematics of both processes are shown in Figure 2.

In the case of radicals, after they are formed, they can proceed to interact directly with other species in the material or form secondary radicals *via* hydrogen abstraction. Various chemical bonds can be cleaved this way, including C-C, C=O, C-S, or C-Cl to name a few. In the majority of cases (but not necessarily always), PI is used for this task. Radical generating PIs can be further classified into type I and type II [44]. Type I PIs generate radicals directly after light absorption, while type II requires the presence of some other constitutes in the material like amines or alcohols. Radicals are then generated after these additional constitutes transfer hydrogen atoms to the PI. Hydrogen abstraction involves aromatic ketone which, after light exposure, forms ketyl radical and donor radical. In those cases, the hydrogen donor radical is responsible for initiating polymerization reaction with ketyl radical couples into a growing polymer chain [45]. As the number of radicals increases, the probability of their collision rises accordingly [46]. After such interaction, radicals are deactivated, and the reaction is terminated. The interplay between radicals can take several different paths. Combination of two active chain results in one long chain. Alternatively, an active chain end can interact with an initiator radical, or radical disproportionation can happen, in which two radicals react to form two different non-radical products by transferring hydrogen from one chain end to the another [47]. Furthermore, radicals can interact with quenchers, for instance, stable radicals, easily reduced or oxidized materials, and salts of some metal [48]. Oxygen also can induce the termination of the polymerization reaction which is exploited in modern stereolithography [49].

In the cation case, after photoexcitation, the charge is transferred to the monomer. It then becomes reactive and can interact with other monomers leading to polymerization. Some of the most popular cation PIs include Brønsted acids such as arenediazonium, diarylodonium, and various sulfonium salts [50]. This is rather problematic in the light of RM as such initiators generate protonic acids that have an adverse impact on cell cultures [51]. In the cationic case, the reaction ends with a combination of an anionic fragment from the counterion with the propagating chain end, as shown in Figure 2.

While in most cases the excitation is discussed in more details, one must not underestimate the importance of termination of polymerization reactions. If polymerization reaction is not properly terminated, it can expand beyond the selectively exposed region, nullifying the intent of spatially selective lithography [52]. On the other hand, smart usage of quenching mechanisms can significantly improve the technology. For instance, first stereolithography machines were based on a resin reservoir with the lowering platform. This required a massive tank of resin to be available at all times, making the whole process less convenient [1]. However, as oxygen is the quencher to most photolithographic materials, in modern 3D printers, structuring is done with only a thin layer of polymer over a transparent, but oxygen access-restricting, window. Then, the printing platform can be raised up out of the resin, and due to quenching, the

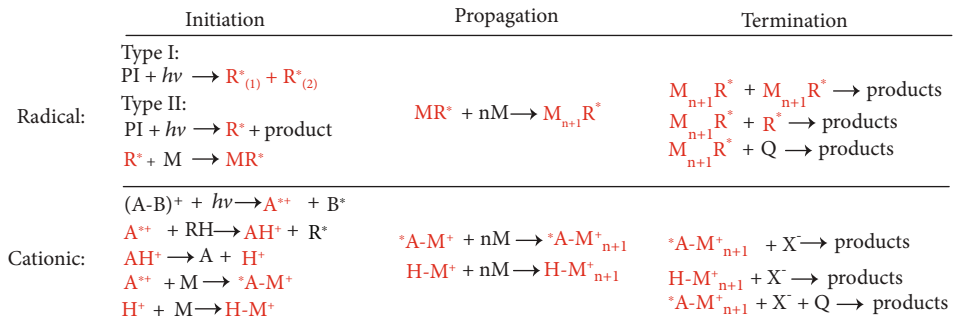

FIGURE 2: Schematics of radical and cation polymerization reactions initiated by one-photon absorption. *hν*: absorbed photon; R* and B*: free radicals; M: monomer; $M_{n+1}R^*$ and $^*A\text{-}M^+_{n+1}$: neutral and cationic macroradicals, respectively; Q: quencher; $(A\text{-}B)^+$: cationic initiator; A^{*+}: cationic radical; AH^+: protonized cation; RH and A: neutral molecules; H^+: proton; $H\text{-}M^+$: protonized monomer; $H\text{-}M^+_{n+1}$: protonized polymer; X^-: counterion. Red markings show the active ingredient that is either causing the reaction or the result of it.

structure does not adhere to the window [49]. For 3DLL, correct control of initiation and quenching is also imperative. Indeed, it can greatly influence the spatial resolution of printing and/or mechanical properties of the final structure [53, 54]. In the light of 3DLL, in RM, the resolution requirements are rather loose. On the other hand, due to the necessity to test exotic materials, correct control of when and where polymerization reaction stops can be very important. Thus, the control of polymerization reaction termination should not be overlooked. However, additional quenching is very rarely used in RM, as it adds additional species to the material that could in some ways compromise biocompatibility. Furthermore, RM structures have, in most cases, features large enough to not require any additional ways to increase printing resolution.

Last, the cross-linking degree must not be overlooked. One of the peculiarities of photopolymerization reaction is the different amounts of photoactive species used, which depends on the exposure parameters. This percent can be somewhere in between ~6% and ~70% depending on the material, excitation, and position in the focal region (decreasing farther from the center) [55]. The last property was employed to generate nanothreads between solid supports. Also, it gives another degree of tunability when considering the concept of the structure [56]. Indeed, refractive index [55], thermal response [13], and mechanical strength [54, 57] depend on it. Consequently, it was exploited in creating various optical and mechanical devices. On the other hand, it means that the characterization of polymers becomes incredibly tricky. Not only must one define what the optical and mechanical properties of the final material are, but also at what conversion degree it was achieved. Therefore, while there will be some characteristic properties of materials listed in this article, one must interpret them with some caution and keep in mind at what exposure parameters it was achieved.

2.3. Fabrication Setup and Strategies. In order to realize TPA, a special workstation is required. In a very generalized case, there are 4 main components in each 3DLL setup: laser source, relay optics, sample positioning, and imaging system (Figure 3). Furthermore, choosing correct writing strategies are also extremely important, because they can influence both the mechanical properties of the structure and the manufacturing throughput. Thus, when considering the capabilities of 3DLL, the hardware/software part of the technology should not be overlooked.

As discussed previously, TPA is a nonlinear process requiring high light I. On a very general level, one can acquire peak I in the focused Gaussian beam by applying the following:

$$I_0 = \frac{2P}{f\omega_0^2\pi\tau}. \tag{2}$$

Here, P is the average laser power, f is the laser repetition rate, $\omega_0 = 0.61\mathrm{NA}/\lambda$ is a radius of the beam waist (NA is numerical aperture), and τ is the pulse duration. As we can see, the laser source is responsible for most parameters leading to high I (P, f, and τ). For this reason, ultrafast fs laser with high P (up to a few hundred mW), reasonable f (which rarely exceeds MHz), and very short τ (tens/hundreds of fs range) is the best candidate to induce it [58]. Nevertheless, picosecond (ps) [59], nanosecond (ns) [60], and even continuous wave (cw) [42] lasers were used for 3DLL. However, in these cases, TPA is surpassed by thermal effects and avalanche ionization as a dominant process for inducing polymerization. This resulted in a decrease in the fabrication window and/or necessity to use a substantially lower translation velocity, thus making ultrafast lasers a primary choice for high-efficiency 3DLL setups. It is interesting to point out that both oscillators and amplified fs laser systems can be used. The latter laser systems are also capable of subtractive laser manufacturing, such as ablation or selective glass etching [5, 15, 61]. Thus, a setup with such laser can perform both additive and subtractive laser processing. While at the moment it has limited uses in RM, it was applied for great effect in other medical fields, for instance, producing functional as lab-on-chip (LOC) devices.

The purpose of relay optics is quite straightforward—direct laser light from laser to the sample. However, peculiarities of this operation should not be overlooked. As established

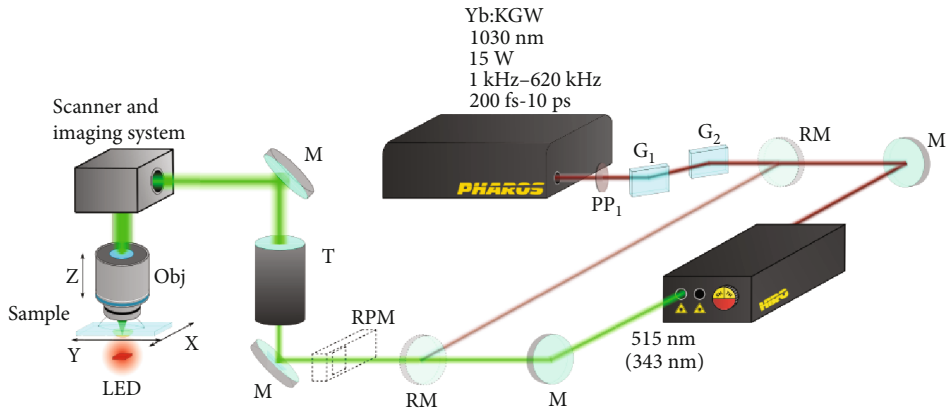

FIGURE 3: Simplified schematics of a 3DLL fabrication setup employing an amplified fs laser and harmonic generator. PP_1: phase plate; G_1 and G_2: Brewster angle polarizers; M: mirrors; RM: removable mirror; RPM: removable power meter; T: telescope; Obj: objective. Adapted with permission from [6] © The Optical Society.

in the last paragraph, laser should be emitting fs pulses. In the case of oscillators, such pulses can be extremely short (sub-100 fs) and, in turn, have relatively broad spectrum width. Furthermore, several laser harmonics might be used in one 3DLL setup [6]. Therefore, optics in the setup have to be able to sustain all of the relevant harmonics with respective spectral widths. In addition, optics have to assure that there is the minimal temporal pulse broadening due to dechirping of the pulse as it passes various optical elements or it is appropriately controlled for the benefit of printing [62, 63]. Alongside spectrotemporal requirements, the optical chain also has to assure that there are no spatial disturbances to the beam. Indeed, to achieve maximal possible writing accuracy, the laser beam has to be as close to Gaussian as possible [64]. What is more, the beam diameter should match the aperture of focusing optics, introducing the need of a telescope. Finally, appropriate NA objective should be chosen to accommodate the needed feature size/throughput compromise [1]. The light intensity in the focal region of Gaussian beam can be defined as

$$I(r,z) = I_0 \frac{\omega_0^2}{\omega(z)^2} \exp\left(\frac{-2r^2}{\omega(z)^2}\right). \quad (3)$$

Here, r is the distance from the optical axis and z is the distance from the focal plane parallel to the optical axis. Because ω_0 depends on NA, by changing the objective, one can relatively easily tune the size of the modified volume. Indeed, in most cases, RM requires relatively big structures (up to cm) with features in the range up to tens of μm [16, 27, 28]. This is substantially bigger than the hundred nm level features possible with 3DLL. Thus, it is common to use objectives with NA < 1 when fabricating structures for RM.

3DLL is realized by moving a focused laser beam in relation to the sample or the sample in relation to the laser beam. On the onset of the technology, piezoelectric (piezo for simplicity) stages were used [65]. They provide extreme precision down to the sub-nm scale. However, their working area is extremely limited (no more than several hundred μm) and translation velocities are limited. They were also sensitive to physical overloads due to the danger of the piezocrystals cracking. These problems meant that piezostages were gradually phased out from the fields where high-throughput printing was necessary, including RM. The next two easily applied options were galvanometric scanners and linear stages. Scanners are a superb positioning tool for very high-throughput fabrication due to the minimal inertia [66]. This means that cm/s translation velocities can be achieved even while fabricating very complex shapes. The downside of this approach is the printing area being confined to a working field of an objective which is in the order of several hundred μm. If structure dimensions exceeded the working area of an objective (which is the case for most RM-applicable structures), it had to be divided into segments which were then printed one by one, resulting in stitching between segments [67–70]. Stitches induce optical and mechanical defects which might compromise functionality of the structure. Linear stages do not have this problem and can produce cm-sized structures at high translation velocities (up to cm/s) if the structure is simple and based on straight lines [71–73]. However, due to the high inertia of the stages, distortions might appear in more complex cases also creating a limitation. The solution to these problems is synchronization of galvanometric scanners and linear stages allowing to achieve stitch-free printing with superb quality of complex 3D shapes at high translation velocities [6]. As a result, it was already used in RM-related research [16].

The final component necessary for practical 3DLL setup is the integrated imaging system. In the simplest case, it is needed to assure that the structure is fabricated at an appropriate position of the sample and for real-time observation of the printing process [72]. At the same time, the functionality of the imaging system can be expanded to include additional roles, such as autofocus. In a general sense, autofocus is needed to find the interface between the prepolymer and substrate. It minimizes the workload on the setup operator and enhances repeatability and precision of such an operation. Depending on the desired result, it can be achieved by using existing imaging hardware and additional image post processing [74] or by introducing more components into the setup [75]. It is important to note that implementation

of autofocus is relatively simple in the 3DLL case due to fluorescence of most processable polymers. This sharply contrasts with finding the interface between two nonfluorescent transparent mediums where more advanced solutions are needed [76].

3. Materials for Multiphoton Polymerization

Alongside the fs laser setup, polymeric materials employed are the most important part of the technology. They define both structuring peculiarities and the characteristics of the produced structures. Therefore, the material has to be carefully chosen, especially in biological structures. Thus, in this part of the review, we will discuss some of the most prominent materials that were employed in 3DLL, as well as PI/inhibitors, and finish off with some ways of functionalizing them.

3.1. Common Photopolymers

3.1.1. Acrylates. Acrylates are one of the most common photopolymer families currently in use in 3D printing. This is due to them being extremely photoactive and chemically tunable. Historically, it was the first polymer structured in 2PP fashion [18]. Acrylates are a family of polymers made from acrylate monomers which are esters. The significant feature of acrylates is that vinyl groups are directly bonded to the carbonyl carbon. These monomers are important due to their bifunctionality. The vinyl group is responsive for polymerization [77]. The carboxylate group carries numerous functionalities providing the ability to modify the composition and chemical structure of acrylates. The polymerization chemistry of acrylates is based on the differences between two vinyl carbon atoms. Usually, vinyl groups are electron rich, while carboxyl groups are very polar. Therefore, the carboxyl group in acrylates attracts electrons from the vinyl group that leads to a deficit of electrons in the alpha carbon and an excess in the beta carbon (Figure 4). This behavior results in the high activity of acrylates in the free radical polymerization reactions described previously.

Many acrylates with a variety of properties can be obtained by changing groups connected to the alpha carbon and carboxylate, for instance, methyl, ethyl, or other organic chain having acrylic, methacrylic, and cyanoacrylic esters [78]. There are abundant acrylate monomers and oligomers that are photosensitive, such as hydroxypropyl acrylate, hexanediol diacrylate, polyester tetraacrylate, hexaacrylate, oxazolidone acrylate, pentaerythritol triacrylate, urethane acrylate, some fluorinated acrylates, and methyl methacrylate [79]. Many acrylates have attractive properties depending upon the chemical structure, such as high chemical and heat resistance, stability, toughness, favorable stiffness, flexibility, optical clarity [78, 80], or 3DLL forming possibility.

It is known that, for instance, in polymethyl methacrylates, the softening point, density, and refractive index decrease and the toughness increases as the ester chain increases. In polymethyl methacrylate, by changing the ester group from methyl to isobutyl, the density can be varied from 1.02 to 1.19 g/cm^3, refractive index can be varied from 1.45 to 1.48, softening point can be varied from 62 to 125°C [78]. On the other hand, if it is necessary to have polymers with special properties, there is a possibility to combine other monomers or modifiers by copolymerization reactions. As a result, the copolymers [78, 81] and blends, also known as acrylic multipolymers [78], are obtained. Some components like ethoxylated trimethylolpropane triacrylate are used in order to reduce shrinkage upon photopolymerization [82]. In order to promote hardness of the polymer, tris(2-hydroxyethyl)isocyanurate should be added [82]. Various modified acrylates were used in 3DLL through the years [83–85]. Overall, acrylate groups play an important role in polymers that will be discussed later, making acrylate chemistry one of the backbones of 3DLL.

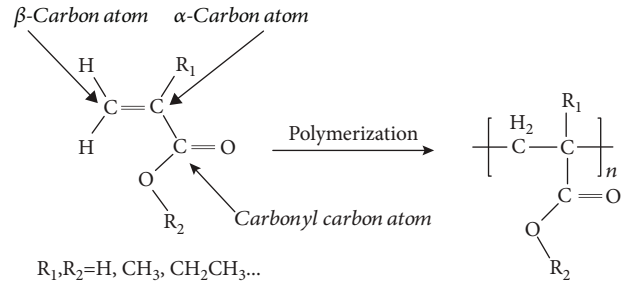

Figure 4: Structural formula of acrylates before and after polymerization. Here R_1 and R_2 are organic substituents and n is the degree of polymerization. Alpha, beta and carbonyl carbon atoms are shown.

3.1.2. SU8. SU8 is a chemically amplified negative photoresin which was introduced commercially in 1996 [86]. It is specially tuned for usage in UV lithography. As a material which was specially designed to be photostructurable, it was natural for it to be applied in 3DLL very early [87, 88]. It is based on the acid-labile groups and the photoacid generator [86]. This results in a rather strict processing protocol. First, it is prebaked to remove the solvent making it hard. It is followed by UV exposure, which generates a strong low concentration acid, for example, hexafluoroantimonic acid from PI decomposes which protonates the epoxides on the oligomer. Such protonated oxonium ions are capable to react with neutral epoxides in cross-linking reactions after irradiation. During this process, the acid also regenerates resulting in a very strong reaction in exposed areas. This reaction is also helped by the fact that in normal circumstances, there are 8 receptive epoxy sites on each monomer (Figure 5). The end result is very well-defined structures that can be relatively big (up to cm) or can have very small features (down to tens of nm [89]).

3DLL processing of SU8 has some interesting features in comparison to the standard UV case. First off, exposure and postbake can be combined into a single processing step [41]. It is possible due to the capability to induce both nonlinear absorption and subsequent heating during the same laser scanning step. The polymerization kinetics are also somewhat different. Raman spectra reveals that when SU8 is exposed to 800 nm, 100 fs, and 1 kHz Ti:saphire, the absorption dynamic is different from the standard UV case. However, the end result is basically the same as SU8 polymerized

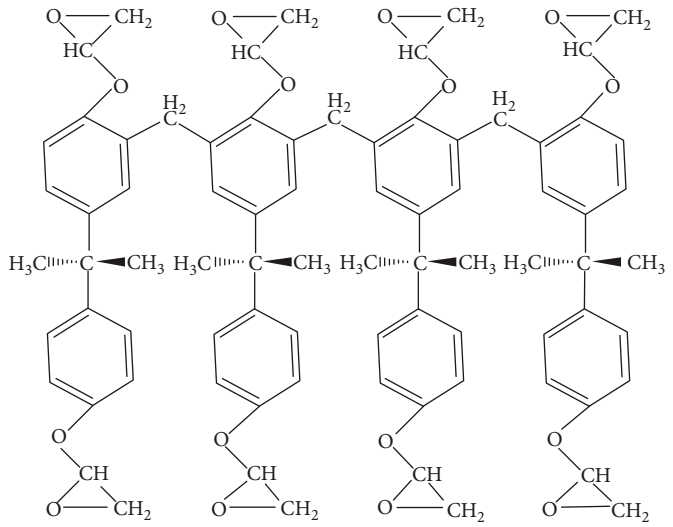

Figure 5: Structural formula of SU8, consisting only of the organic matter.

with UV light and TPA has nearly identical Raman spectra [19]. Both subdiffractive structures [88] and mm scale objects [90] were fabricated using 3DLL out of SU8. Due to relatively good adhesion of SU8 to various functional substrates, structures can be printed directly on them. One of the examples is fiber tips [91]. SU8 consists only of the organic matter; therefore, it can also be removed by calcination in ambient atmosphere in rather low temperature of 600°C, making it a good candidate for the template material for other substances that are hard to shape in 3D directly [92]. Interestingly, SU8 usage in medicine is rather sparse, especially in the 3DLL case. This can be explained by the fact that other materials are more customizable, biodegradable, and/or bioinert. However, it is still a potent candidate if structures with well-defined and mechanically strong features are needed.

3.1.3. Hydrogels. Hydrogels can be described as the polymeric networks which have the ability to take and storage an extremely large amount of water in their 3D structures. The reason for this is a chemical structure of material. The hydrogels are formed by hydrophilic groups which are hydrated in an aqueous medium [93, 94]. Generally, hydrogels are insoluble in aqueous solution because of polymeric cross-links. Nevertheless, because of the large quantities of water due to the hydrogen interactions inside the polymer network, these materials exhibit the capability to swell in aqueous solutions [94]. As a result, chemically hydrogels can be defined in two conditions: one of them is the water-insoluble polymeric chain and the other is the hydrophilic functional groups.

The two requirements described above lead to a wide variety of hydrogel precursors. In order to facilitate understanding of hydrogels, they are classified in many aspects. According to the hydrogels origin, they can be classified to the natural or synthetic polymers. Furthermore, the classification based on polymeric composition allows grouping hydrogels into homopolymeric, where a basic structure consists of a monomer, and copolymeric—of two or more different monomer species with one hydrophylic component and multipolymeric interpenetrating polymeric hydrogels consisting of two independent cross-linked polymers. Furthermore, hydrogels can be classified according to crystallinity, for example, amorphous, semicrystalline, or crystalline. Also, based on polymeric chains and the electric charge of hydrogels, they can be grouped into nonionic, ionic (that include both cationic and anionic), amphoteric (with acidic and basic groups), and zwitterionic (including both anionic and cationic groups) [94].

However, not all hydrogels can participate in photopolymerization. In 3DLL, precursors of hydrogels are usually liquid and should immediately respond to irradiation of light. Therefore, PIs which accelerate photopolymerization reactions are necessary. Multifunctional cross-linkers, such as acrylic acid or (meth)acrylates, create links between the polymeric chains. Frequently, monofunctional reactive dilutes are added in order to adjust the viscosity [26]. Photopolymerizable hydrogel precursors could be HA-MA/acrylamide, modified gelatin, collagen, fibrinogen, fibronectin, concanavalin A, lyophilized BSA (bovine serum albumin), BSA, PEGda/-HEMA, and so forth, together with eligible PIs [26]. One of the most used hydrogels for several decades is PEGDA [95, 96]. Its structural formula is depicted in Figure 6. PEGDA consists of polyethylene glycol with two acrylate substituents at the ends of the chain. PEGDA is functionalized by polyacrylic or polymethacrylic acids in order to form cross-linked hydrogels. These compounds have an oxygen atom in a polyethylene glycol part and carboxylic group in an acid part. The hydrogen bond between these groups is formed. This behavior depends on pH, because the reason for hydrogen bond formation is the protonation of the carboxylic group [93]. However, properties of hydrogels can be changed not only by changing pH properties. Various factors, such as temperature, pressure, solvent composition, or ion changes, can control them, including cross-linking density, hydrophobicity, swelling rate, permeability, degradability, and mechanical strenght [26], of gels which are

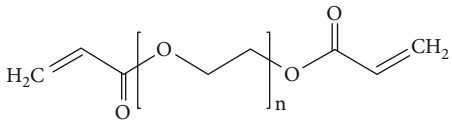

Figure 6: Structural formula of polyethylene glycol diacrylate (PEGDA). Here, n is a degree of polymerization.

important for the 3DLL process and for the applicability of the final product.

Biocompatibility is one of the key properties of hydrogels that make them attractive and promising in RM. The ability to polymerize them with 3DLL further extends their applicability [26]. Indeed, from most of the currently available materials, they offer one of the best analogs for the extracellular matrix. Thus, numerous different structures were created out of hydrogels over the years using 3DLL [20, 72, 97, 98]. Their peculiarities will be discussed in more detail further in this article.

3.1.4. Hybrid Organic-Inorganic Photopolymers. With the advances of polymer chemistry came the possibility to add a lot of different functional groups to the cross-linkable monomers. One of the key achievements in the field is the possibility to prepare hybrid materials that are cross-linked *via* organic constitutes yet have diverse and significant inorganic part. In most cases, they are prepared by sol-gel technology [99, 100]. The sol-gel synthesis method includes a powerful and adjustable strategy for the preparation of functional organic-inorganic hybrid materials. It provides easy control of the configuration of the materials as well as molecular composition that permits hybrids more applicable to fundamental or applied research and industry. The sol-gel chemistry is based on hydrolysis and polycondensation reactions of suitable molecular precursors such as metal alkoxides M(OR)x [101, 102], where M is the metal or metalloid element, for instance, Si, Sn, Ti, Zr, Hf, Ge, Al, Mo, V, W, and Ce [103], while R is the alkyl chain or any other organic group. The possibility of using metalorganic materials in 3DLL requires one important condition of the alkoxide organic group—one or more organic groups must have a functional group involved in photopolymerization reactions. Therefore, in 3DLL, a silicon-based metalorganic monomer (MAPTMS, TEOS, TMOS [103], or other silane) is used together in the presence or absence of another metal isopropoxide which is usually stabilized by methacrylic acid (Figure 7). The sol-gel method provides the opportunity to synthesize homogeneous materials with the degree of mixing of the organic-inorganic components and a variety of metals that allows a variation of its appealing properties such as molecular homogeneity, transparency, flexibility, and durability [103]. As mentioned above, the hydrolysis and condensation reactions of monomeric metal alkoxides and organyl alkoxides are the two main stages of sol-gel synthesis [104]. In solution, the alkoxides are hydrolyzed and condensed to form polymeric species composed of M-O-M bonds [102, 105]. Both reactions occur by acid- or base-catalyzed bimolecular displacement reactions. The acid-catalyzed mechanisms are carried on protonation of OH or OR substituents attached to silicon or other metal element, whereas under basic conditions, hydroxyl anions attack metal or the metalloid element directly. Both reactions occur simultaneously and, depending on reaction equilibrium, start to form three-dimensional inorganic molecular networks. The geometry and length of condensation bonds strongly depend on catalysts, steric and inductive effect of the alkyl radical, and solvents [105]. Such hybrids with different composition and diversity of geometry are promising materials for various applications.

Hybrids offer huge tunability in terms of mechanical and optical properties by changing the ratio between the organic and inorganic parts. For this reason, they become extremely popular in 3DLL. Indeed, hybrids with Si [21], Zr [106], Ge [107], and Ti [108] constitutes were tested over the years to name a few. However, they vary heavily in terms of ease of preparing them, shelf life, and general structurability. This led to Si- and Zr-based hybrids becoming the most popular ones. Zr-based hybrids are especially interesting as they were created on purpose for use in 3DLL and offer minimal shrinkage [106]. Zr based initially created with the intent to use it in photonics [106]. Nevertheless, over the years, it was used in basically all research areas where 3DLL can be applied, including photonics [9], microoptics [109], and micromechanics [110]. It was also proven to be exceptionally susceptible to modification, including surface tuning [10] or doping with organic dies [6, 111] or nanoparticles [112]. In RM, the Zr-containing hybrid was employed in the manufacturing standard [16, 73] and shape-shifting scaffolds [113] as well as functional elements such as valves that could be used as implants replacing analogous elements in veins [110]. Biological use of the Zr hybrid is heavily motivated by the superb biocomaptability of the material, proven both *in vitro* [73] and *in vivo*, going as far as preclinical trials [16].

3.1.5. Elastomers. As the name implies, an elastomer is an elastic polymer. It owns this property to relatively weak intermolecular forces, low Young's modulus (~MPa), and relatively high failure strain. Most of the elastomers are cured using heat, making them very convenient for technologies such as fast replication [114] or microfluidics [115]. While numerous elastomers were created and tested over the years, one of the most popular is the commercially available polydimethylsiloxane (PDMS) (Figure 8), which is sold under the name Sylgard® 184. Furthermore, more monomers were studied by researchers, such as elastomers in photopolymerization. Alongside appropriate monomer reactive, diluents and chain transfer agents [116] are needed too. In the PDMS variant, such a system may consist of MMDS ((mercaptopropyl)methylsiloxane-dimethylsiloxane copolymer) which is oxidized by adding different amounts of the IBDA (iodobenzene diacetate) solution, vinyl-terminated PDMS, PI, and photoabsorber [117]. In other systems, some acrylates may be used as the base monomers. These include aliphatic polyester urethane diacrylate, urethane monacrylate in 20% EHA and aliphatic urethane acrylate oligomer, as reactive diluents such materials as 2-(((butylamino)carbonyl)-oxy)-ethyl acrylate, 2-ethylhexyl acrylate, 2-hydroxyethyl acrylate, and 2-cyanoethyl acrylate. As the chain transfer agents, the

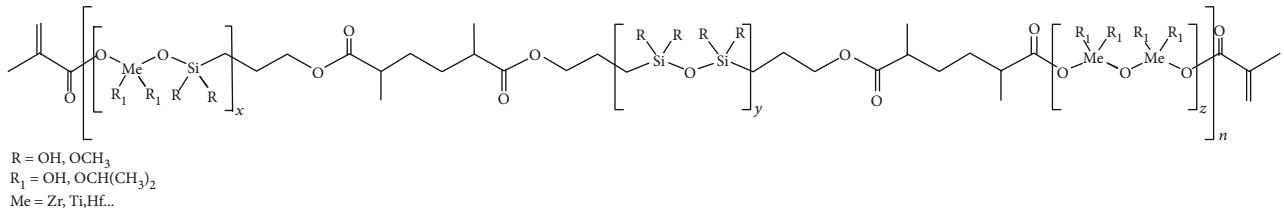

Figure 7: Structural formula of hybrid organic-inorganic polymer consisting of MAPTMS and metal isopropoxide. Here x, y, and z are degrees of inorganic polycondensation.

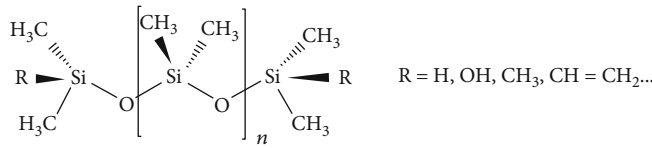

Figure 8: Structural formula of polydimethylsiloxane oligomer (PDMS). R is organic substituent at the end of the chain and n is a degree of polycondensation.

pentaerythritol tetrakis(3-mercaptopropionate), and 3,6-dioxa-1,8-octane dithiol are applied [116]. The reagent names indicate that acrylates are the inseparable part of elastomers. However, it should be noted that only a small part of acrylates can exhibit elastomeric properties.

Medical applications are one of the areas where elastomers show huge promise. Here, they excel due to their biocompatibility, capability to pass through gas while retaining liquids and being generally transparent to visible and UV light. One of the areas where it was exploited heavily was LOCs [115]. Cells could live in biological liquids contained in such devices, while also being able to "breath." Transparent nature of elastomers also allows easy assessment of such biological systems. Biooriented scaffolds made out of various elastomers and their composites were also produced for RM applications [118–120].

The importance of 3D nanostructuring of elastomers was recognized very early in 3DLL. However, while 3D structuring of PDMS was achieved, it was done in very slow 100 ms/voxel exposure [121]. In further works, the speed was increased from tens [122] up to thousands [123, 124] μm/s, but the problem of the narrow fabrication window and shrinkage remained. Due to their elasticity and polymerization post-fabrication, the shrinkage remains one of the main problems of 3DLL-compatible elastomers, even if special purpose-built species are used [124]. Thus, while 3DLL structuring is possible and materials are RM compatible, they are not easy and straightforward to use.

3.1.6. Biopolymers. Ever increasing material synthesis capabilities led to the creation of polymers similar to ones found in nature (for instance, synthetic proteins) or based on naturally derived raw materials. Due to these connections, in this review, we will consider both of these types of materials to be biopolymers. Their main attraction is the possibility to extremely closely mimic the biological environment, use readily available natural raw materials, or both.

In a world with dwindling oil resources and ever growing consumption of energy, alternatives for oil-based polymers are highly desired. Naturally derived raw material-based biopolymers are designed to answer this challenge. The polylactic acid (PLA) is one of the first polymers of this kind to be commercialized. Based on corn, it offers an extremely low price (~several dollars for kg) and easy handling [125]. It also shows favourable degradation properties [125, 126]. Both additive [127] and subtractive [128] manufacturing were achieved with PLA. Yet it and other associated biopolymers were rarely used in photolithography due to the difficulties in additive photostructuring. Movement to photolithography requires to tune both monomer formulations and choose the correct PI. It was shown that standard one-photon polymerization might be tricky and hard to use [52]. Interestingly, when moving to TPA, some of these problems are significantly reduced [129]. This might be related to a lot more aggressive and localized energy introduction mechanism in the 3DLL case.

Talking about biomimicking polymers, several kinds were tried over the years, including protein [130, 131], collagen [132], chitosan [22], and gelatin [133]. However, most of these materials are not easy to structure *via* fs lasers. Species with special PIs and even ones without were tried with varying degrees of success. In some cases, deformed, barely standing 3D structures were demonstrated with intent to showcase the possibility of such processing. In other cases, well-defined and usable 3D objects were manufactured. Overall, this area is relatively new, and a lot of advances in further developing biopolymers for 3DLL might be expected.

3.1.7. Positive Photoresins. All photopolymers discussed so far are of the so-called negative tone kind. It means that areas which were exposed to the light are cross-linked and remain after the development. However, the opposite can also be realized by using so-called positive tone resists. In that case, under irradiation, exposed regions of photosensitive material are removed during development. Typically, positive resists consist of a polymer matrix with protected functionalities, small molecular photoactive generator, solvent, and other additives [134, 135]. One of the most

significant requirements of these systems is photosensitivity of the photoactive generator which is basically called a photoacid generator due to its property to produce acid after the light irradiation. The photoactive generators can be divided into two types, first is the ionic, which mostly contains onium salts and upon UV light is able to produce Brønsted acids, while the second type is nonionic that can generate sulfonic, carboxylic, and phosphoric acids. Generally, polymers having tertiary carboxylate, tertiary carbonate, tertiary ether, acetal, hemiacetal ester, or other easily protonizable group are used in positive tone resist systems. In that case, after the photoactivated acid-catalyzed reactions, such polymers are decomposed into poly-carboxylic acids or poly-phenols [134], depending on the initial functional group, and the smaller molecular weight having nonpolymeric compounds. Thereafter, polymers having acidic functional groups can easily dissolve in an alkaline solvent. The described system is called the amplification resins.

But what if the polymer does not have an easily protonizable functional group? The most prevalent type of positive tone photoresist consists of diazonaphthoquinone (DNQ), phenol formaldehyde polymer (Novolac), and propylene glycol monomethyl ether acetate (PGMEA) as the solvent [136–139]. In this way, at normal conditions, the dissolution of the polymer is blocked by the hydroxyl group of Novolac and DNQ interactions. However, after the photoillumination, indenecarboxylic acid is formed via ketenes [136] of the DNQ; as a result, the Novolac polymer becomes soluble [140].

Positive tone resists were applied in 3DLL [141] with the primary focus on the possibility to use them in microfluidics [142]. However, due to their nature, they are relatively chemically unstable with short shelf life and narrow fabrication window. Thus, in recent years, they were used less and less in favour of easier to use and applicable negative tone resists.

3.2. Photoinitiators in Regenerative Medicine. The correct choice of PI or photoexcitation mechanism is imperative for 3DLL. In most cases, a specific PI is used for it. PI's influence to the whole printing process is immense because it determines what laser wavelength should be used and what is the fabrication window. When 3DLL was first used, photopolymers with PIs designed for one UV photon absorption were applied due to being readily available [18, 121]. From the first glance, it might seem that adoption of one-photon PIs for TPA should be pretty straightforward by just making sure that the fs laser wavelength is half of the absorption peak of the PI. However, interestingly enough, it was shown that sometimes PIs with huge one-photon absorption cross-section σ_1 can have very small σ_2 in the range of tens of GM [143]. In comparison, if appropriate chemistry is used, σ_2 can go as high as more than a thousand GM [143]. This proves the necessity to create PIs specially designed for TPA.

TPA-oriented PIs can be realized by applying D-π-D, D-π-A, D-π-A-π-D, and A-π-D-π-A types chemical compounds showing large changes of dipole/quadrupole moments upon excitation, with extended conjugation in molecules [144]. Here, π is a π-conjugated backbone (for example, vinyl groups in ethynylphenyl, ethynylene, or phenyl); D usually represents hydrogen, methoxy, and alkylamino, such as dimethylamino, diphenylamino, and dibutylamino groups which act as electron donators; and A is the acceptors (for instance, various cycloketones, ketones, pyridine, or pyridinium) [144–146]. D-π-D and D-π-A-π-D are two of the most commonly used PI systems in TPA. One of the D-π-D type, commercially available PIs, which is known as Irgacure 2959, could have attractive properties for medicine application as PI, due to its biocompatibility and solubility in water [145]. However, it is only appropriate to the 515 nm wavelength, which may cause the denaturation of proteins, which is critical when processing in the presence of cells [145, 147]. Therefore, D-π-A-π-D system PIs are more attractive in medical applications due to the charge transfer between electron donor (D) and acceptor (A) groups which are responsible for the appearance of low-energy excitations [148], such as 800 nm [146].

If the final structure is expected to be used in RM PI, despite the discussed necessity of low energy excitation, it must match even more requirements. First, it has to be biocompatible. This can be tricky, because PI molecules are purposely designed to be extremely chemically active resulting in possible cytotoxicity [95, 149]. It is known that the cytotoxicity is determined by singlet oxygen quantum yields during photoinitiation. In the case of D-π-A-π-D, cytotoxicity was found to be influenced by the composition of the activator. The smaller number of C atoms in the cycle of cycloketones (at least from C4 to C7) showed the less amount of the singlet oxygen quantum yield [150]. Furthermore, they have to be water dissolvable. This requirement stem from the desire to use water-soluble hydrogels in RM and potentially avoid organic solvents in development process. It was shown that some standard PIs can be biocompatible as long as they are used in inert hard polymer matrices, such as hybrid organic-inorganic photopolymers [16, 73, 113]. Purpose-designed bio-PIs were also developed. In order to achieve water solubility, water-born functional groups can be introduced. These can be, for instance, quaternary ammonium cations or carboxylic sodium salts. Biocompatibility of such water-soluble PIs was proven by both seeding scaffolds with cells and printing structures with whole organisms. It was shown that such bio-PIs can have σ_2 high enough to support printing speeds well over cm/s [151]. Therefore, the selection of PIs suitable for RM is quite big, fully supporting the growth of the technology.

As mentioned above, another important requirement of PIs is the sufficient two-photon absorption cross-section value which is most dependent on the chemical structure, hydrophilicity/-phobicity, and solvent. According to Albota et al., the two photon absorption cross section increases due to the increasing conjugation length of the molecule or the increasing extent of symmetrical charge transfer from the ends of the molecule to the middle or vice versa [152]. Furthermore, with the hydrophilic PI P2CK (Figure 9) under 800 nm excitation in water, the TPA cross-section value was equal to 176 GM, while its hydrophobic analogue (B3FL) in chloroform was 466 GM [153]. The hypothesis of such behavior is interpreted by hydrogen bonding between the solute and solvent and changes in the PI geometry or aggregation [145].

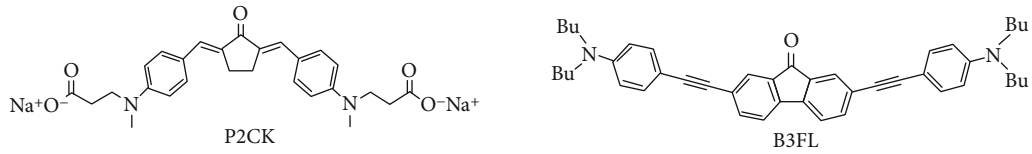

Figure 9: Structural formulas of TPA PIs. Here, P2CK is PI-soluble in water, while B3FL is soluble in organic solvents.

While PIs are the primary way to induce cross-linking, it was also shown that in some cases, polymerization reaction can be induced even without PI present [2, 133, 154]. This potentially eliminates the need to use PI and, thus, optimize its printing and biocompatibility-related properties. On the other hand, it reduces the fabrication window, potentially weakens the structure mechanically, and creates additional requirements for the light source [154]. This is due to the change in the undergoing light-matter interaction. It was calculated that if PI is not present, avalanche ionization might become comparable or an even greater contributor to chemical bond cleavage than TPA [40]. However, as the avalanche requires time to achieve its full potential, relatively longer pulses in the range of hundreds of fs are necessary. Another way to achieve PI-less structuring is to specially design the material to have double bonds breakable directly by TPA [133] (Figure 10). Then, the material acts as polymer and PI. PI-free structuring alongside bio-PIs make selection of photosensitization mechanisms very broad which is extremely suitable for such a subtle field as RM.

3.3. Material Functionalization and Modification. In a lot of cases correct choice of the polymer and PI is sufficient to satisfy the needs of the application. However, in some special cases, further modification of the material might be desired. Due to the extreme flexibility of 3DLL, a lot can be done to the polymers used while retaining the possibility to structure them in 3D fashion.

3.3.1. Organic Modifications. Polymeric matrix might be enhanced by using organic additives. These might serve several functions. First, these additives might be various biological or curing agents that are released as the biodegradable polymer dissolves in a living tissue or bioliquid [155]. If the scaffold is produced out of such material, it both supports the cell growth and potentially provides cure for the trauma/-disease in its proximity. Second, additional organic dyes can be added [6, 111]. It makes structures easier to see in either ambient lighting or under UV light. This is attractive for medical applications if nondegradable scaffolds need to be observed or removed. However, as with the PIs, care should be taken to make sure that such dyes are not cytotoxic if application is biology oriented. Also, the absorption of the dye needs to be considered and 3D printing performed with laser wavelength for which such material is transparent [6].

3.3.2. Inorganic Modifications. The problem with organic fluorescent dyes is their bleaching overtime under UV radiation. If long-term emission is needed, inorganic additives are superior. In that case, 3DLL-applicable polymers can be mixed with various inorganic nanoparticles and quantum dots. Indeed, by controlling the shape and size of such nanoobjects, their absorption and emission characteristics can be changed from UV to IR wavelengths [156, 157]. In the 3DLL case, they can be introduced into polymer either after printing [158] or just by mixing them into prepolymer before printing [112, 159, 160]. The second option is extremely attractive due to its simplicity and is always used if possible. Alongside well-controlled absorption/emission characteristics, nanoadditives can also be used in other ways. For instance, they can be used as PIs. With very small concentrations needed (~10^{-3}% w.t.) and comparable photoactivation to standard Pi [112], gold nanoparticles are promising in biological applications as a replacement for standard PIs. Finally, enhanced and/or controlled photosensitivity can be realized with other nanoadditives such as ZrO_2 [161] or upconverting lanthanide-doped upconversion materials [162]. Thus, this approach can be considered to be extremely versatile and applicable to multiple materials.

Modifications using inorganic additives extend beyond just a control of photosensitivity. Quantum dots can also be used to modify the mechanical and optical properties of the nanocomposite beyond what could be achieved with only polymer chemistry [159] (Figure 11(a)). Furthermore, magnetic properties can be introduced to the polymer *via* magnetic nanoparticles [163]. Alongside 3DLL-enabled conductive nanocomposites [164], it creates a precedent for the completely controllable electromagnetic properties of the structure. This is extremely relevant for RM as some tissues rely on electric conductivity of the surrounding medium. At the same time, it would enable printing miniaturized active implants such as heart simulators or microrobots. Therefore, nanoadditives and resulting nanocomposites are an extremely important area for development with huge promises to 3DLL overall and with interesting implication to RM in particular.

3.3.3. Postprocessing Solutions. In its essence, 3DLL is only capable of printing polymeric materials. While polymers can be tuned in extremely diverse ways, there are properties that are nearly unreachable with polymers. Thus, ways to expand additive laser 3D manufacturing beyond polymers exist. Recent works showed that one of the best ways to achieve free-form 3D nanomanufacturing of inorganic materials is combining 3DLL and thermal postprocessing [154, 165–167]. The usage of this methodology can lead to several outcomes. Heat might be used to remove organic polymer completely. Then, it can be used as a mold for a material that could not be directly structured *via* 3DLL, for instance, metal [168]. The end result in such a case is high-quality metallic micro- and nanostructures. In a similar fashion, heat can also be used to directly form inorganic structures. Then, the 3D

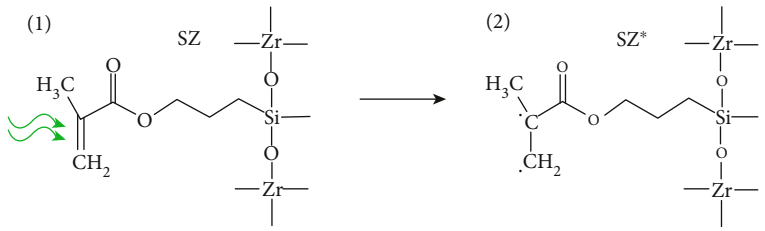

Figure 10: Proposed interaction in the acryl group in hybrid organic-inorganic photopolymer SZ2080 (SZ) during PI-free cross-linking. Direct cleavage *via* nonlinear absorption of a double bond in a group results in radicalization and subsequent polymerization. Adopted from [154].

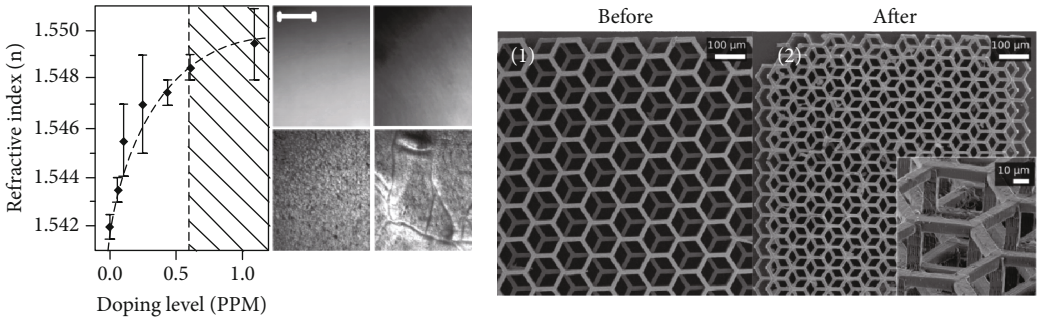

Figure 11: (a) Refractive index change and structure topography of material doped with different concentration of PbS quantum dots. Substantial change of both is clearly visible. Scale bar: 50 μm (adopted from [159]). (b) Scaffold structure made out of hybrid organic-inorganic photopolymer SZ2080 (1) and then modified into glass-ceramic *via* thermal postprocessing. Clear downscaling while preserving the shape and structural complexity is evident (Adapted with permission from [166] © The Optical Society).

structure is produced by using 3DLL using hybrid organic-inorganic photopolymer or similar mixture. Postprocessing is then used to remove most of the organic constitutes leaving inorganic 3D structure. As an added bonus, during this process, a substantial downscaling of a structure occurs—up to 21% of initial size in the 2D line case [165] and 60% in the 3D case [154]. The shrinkage was observed in both nanolatices [154, 165] and bulk 3D structures [166, 167]. It is also completely isotropic in all directions making it very predictable [166]. Thus, it was used to produce even extremely complex 3D microstructures [166, 167] (Figure 11(b)). A method of this kind was already shown to have huge promise in producing true 3D glass microfluidic systems [169]. While it was not applied in RM, so far, the possibility here would be to produce ceramic implants that could well mimic bone or teeth. Scaffolds of required geometry and overall size were already demonstrated with possible further works in RM direction in the near future.

Finally, surface modifications should not be overlooked. It was shown that correct surface topography and chemistry has immense impact on the functionality of medical implant. Functional groups like carboxylic acid groups, hydroxyl groups and amine groups generally produced by plasma treatment are used to chemically functionalized polymer surfaces. In the case of 3DLL-made structures, such as scaffolds, surfaces can be functionalized by plasma treatment for acrylic acid surface polymerization and further grafted with laminin-1 or gelatin in order to enhance human cardiac progenitor cell (CPC) survival and differentiation potential [170]. Furthermore, surface properties which are significant in medical application, such as adhesion, surface hardening, surface wettability, tribology, blood compatibility, and diffusion barrier, can be obtained by functionalizing polymeric surfaces with organic materials. For example, superhydrophobic materials are obtained by using tetrafluoroethylene or 1H,1H,2H,2H-perfluorooctyl acrylate precursor plasma polymerization. Also, in order to make blood-compatible surfaces, the hexamethyldisiloxane can be used to reduce loss of blood cells through blood contact. For the thermal resistance and electrical properties, a polymer can be functionalized by covering of cyano groups [171]. At the same time, conductive and/or magnetic coating can be selectively deposited on 3DLL-made objects. Then, the metallization process is based on three stages. The first stage is seeding of metal, such as silver, when the 3D structure is immersed in an aqueous solution of silver nitrate ($AgNO_3$), where silver ions connect together with amine moieties, which are only on the polymeric structure's surface, thus forming the initiation of the silver nanoparticles growth. In the second step, metal ions are reduced, in this case, by aqueous solution of sodium borohydride ($NaBH_4$), and silver nanoparticles are formed. The amount of silver plated onto the structures depends on the duration of these stages. Finally, during the plating, the structure is immersed in the reducing agent to form a smooth final layer of metal [10, 172, 173]. The result is a metal layer just only on 3DLL-made structures. This was shown to lead

to conductive 3D structures [172] or plasmonic functionality [10]. Magnetic interaction-based cell transportation was also shown [173]. In medicine, this can be relevant as a way to introduce electricity to various electromechanical implants or simulators.

4. Applications in Regenerative Medicine

In order to achieve the final goal of RM, a lot of different, separate, yet intertwined research topics have to be investigated. Living cell behavior on different materials and geometrical topographies have to be onsidered. These results have to be compared to true living tissues. Novel designs for RM-oriented structures then have to be developed in accordance to obtained results and precise medical needs. Then, overall body response to printed objects have to be known as the final goal of the RM is to have structures and methods that could be used in the human body. All of these directions are being tackled with the help of 3DLL.

One of the key backbones of RM research is scaffolds for cell growth and tissue engineering [174]. They allow both investigating cell behavior in different conditions and being used for curing damaged tissue. When creating scaffolds, a lot of different considerations have to be taken into account. The 3D aspect is especially important here. While a huge array of cell-related research was performed with 2D structures [175–177], the extent of capabilities to mimic living body in 2D environments is limited. Thus, 3D objects are required for any high-level research. Diverse methods were used to fabricate scaffolds. Some of them are considered passive and include phase separation [178], porogen leaching [179], gas foaming [180], freeze-drying [181], and electrospinning [182]. The key advantage of these methods is the capability to create scaffolds for virtually any synthetic or natural material. Furthermore, the feature/pore size in such structures can be tuned to be in the range of what is found in natural ECM. This is extremely important in RM, as ECM influences cell behavior in a variety of different ways, including their proliferation, migration, or mass transportation. However, all of these methods are to some extent random in nature, making predetermined scaffolds with precise architecture nearly impossible. Here, various 3D printing techniques show huge advantage due to structure on-demand capabilities [183]. However, from all of the standard 3D printing techniques available today, only 3DLL have the correct blend of achievable resolution and acceptable throughput [1].

3DLL-made scaffolds were used in a huge variety of ways to investigate the peculiarities of cell and printed structure interaction. Specially designed wells with channel-like structures were applied to investigate the peculiarities of neuron growth and connection, showing that directionality of surrounding structures is extremely important [184]. Also, pore size in the scaffold can have huge implications to cell migration and mass transportation [185] (Figure 12(a)). Even if gaps in the scaffold structure are smaller than the cell itself, the macromolecules can still pass through such barrier [186]. Understanding these mechanics is imperative in creating scaffolds that are custom tuned to allow certain cell migration and, at the same time, unrestricted communication between cells. Cell adhesion is another important topic. Biochemistry behind the cell-ECM interaction is extremely elaborate. Some materials might have superb cell adhesion while others might repel the cells. The first effect was shown to be extremely useful when controlling cell attachment points in a specially designed scaffold having functionalized points made out of bioactive species on top of the inert scaffold. This can be further expanded to include both repelling and attracting species in a single scaffold [17]. Then, the four-sided supports are printed out of a basic hydrophilic resist, consisting of a mixture of commercially available components: a trifunctional acrylate as the network-forming species (trimethylolpropane ethoxylate triacrylate, TPETA) and a PI (Irgacure369), with a functional photoresist, which has protein- and cell-repellent properties along with a photoreactive component that can be activated by DLW in order to change its properties to attract protein binding; as a result, protein-binding surfaces are obtained on the cross-beams. Such resist is obtained by mixing previously described basic resist (TPETA) and a methacrylate containing either a phenacyl sulfide (PS) or an o-methylbenzaldehyde (photoenol precursor) (PE) part. Finally, the inorganic-organic hybrid photoresist OrmoComp is used as a third resist providing an inherent protein-adhesive surface on the opposite cross-beam ends of the scaffold. Subsequent UV light leads to biotinylation of the functional resist cross-beams, making them either attracting for specific binding of the vitronectin. Due to the passivating properties of both basic and biotinylated resists, fibronectin on laminin only bind to the OrmoComp beams. In this particular case, epithelial (A549) and fibroblast (3T3) cells were chosen: the first kind has good adhesion to OrmoComp-laminin cross-beams and is repealed by the vitronectin, while the second type has completely inverted adhesion-repulsion properties [17]. As expected, cells were shown to attach to a preferential material proving that 3DLL can be employed for complete tissue engineering, starting with the completely freely definable 3D geometry and on-demand chemical functionality all done in the size range that can be smaller, bigger, or the exact cell size.

Having good knowledge about cell-scaffold interaction, scaffolds can be applied directly for treatment purposes. Here 3DLL can be used in a huge variety of ways. For instance, scaffolds might be used as a breeding platform to acquire cells for various cell-based treatments [73] (Figure 12(b)). Then, relatively simple geometry scaffolds with pore sizes optimized for the particular cell type can be made. Such colonies can be up to mm in size, making the entire amount of growth chambers in the range of tens or even hundreds. Furthermore, it can induce the genetic reprogramming of the cell, once again showing the importance of the scaffold shape and subsequent cytoskeletal tension in the cell [187]. While direct cell therapies have huge promise, in some cases, movement of the liquids in the body might destroy new cell colonies. A primary example is the blood flow in the cardiovascular system. Then, more rigid scaffolds can be applied to keep cells in place [71]. Then, the question of biodegradability arises.

Sometimes it would be desired that after cells are self-sufficient, the scaffold would degrade and entirely normal tissue

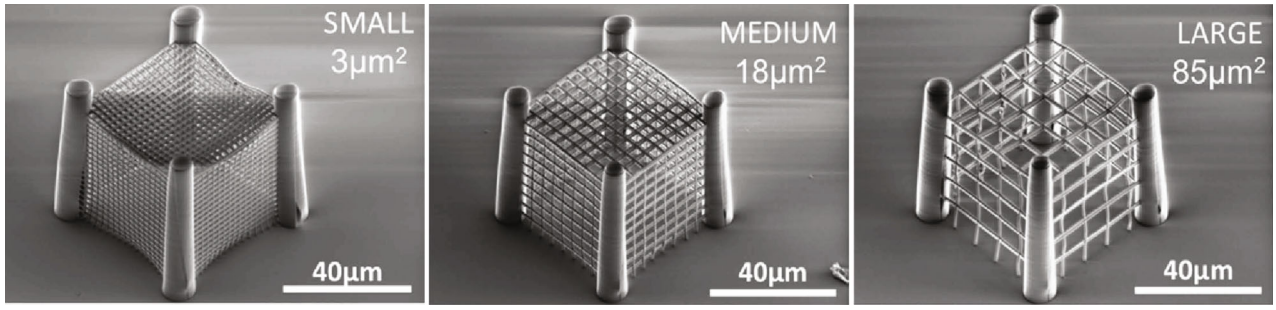

(a)

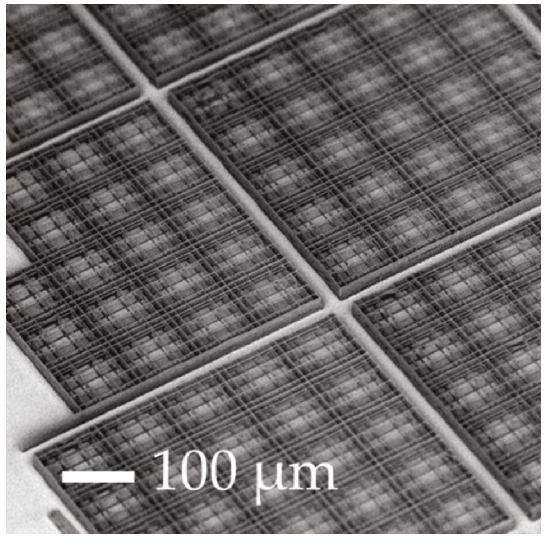

(b)

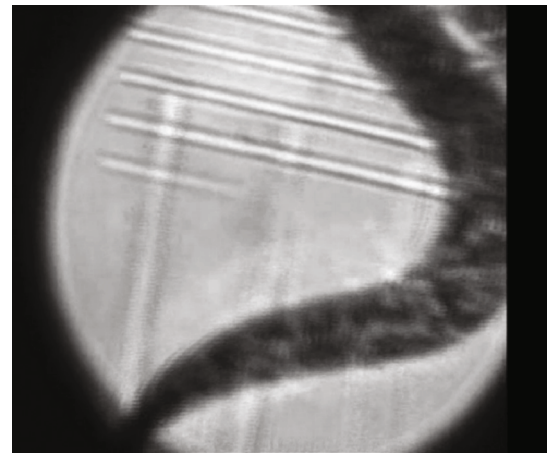

(c)

Figure 12: (a) SEM images of 3DLL-made structures with varied pore areas used to test cell interaction in scaffolds which might be smaller than the cell itself [186]. (b) Supermatrix of nichoids as a cell culture containing 218 matrices at a distance of 30 μm. Such structures show clear capabilities of 3DLL to be employed at mass production of biological scaffolds [73]. (c) Real-time view *via* setup imaging system depicting the writing of a scaffold in the presence of a living *Caenorhabditis elegans* showcasing that 3DLL combined with a biopolymer can be completely biofriendly and does not have adverse impact on living organisms [72].

would grow [188]. On the other hand, in some cases, nondegradable scaffolds are also acceptable. For instance, they could be employed in bone regeneration where they outperform modern cologne membranes [16, 189]. The middle ground between degradable and stiff scaffolds is shape-shifting structures [113]. 3DLL can be employed to print burr-like structures that could later be seeded with cells. Due to relatively small size and hooks on the outside, such balls can then be applied to the wound as a gel. It then mimics the shape of the wound. The freedom of geometry is a massive enabler in RM, and one could expect only more precisely tuned or nontrivial geometries to be used.

Most of the research conducted so far was performed *in vitro*. Results acquired in this manner are extremely important for the development of the field. However, *in vivo* applications need to follow. So far, several works were done in this area. For example, a 3D structure was printed in hydrogel in the presence of the whole organism [72]. The *Caenorhabditis elegans* used in this work was shown to not only survive in photoactive hydrogel but also live through the printing process (Figure 12(c)). This again shows that the cold nature of fs processing is extremely attractive in RM. Keeping in mind that 3DLL can be realized through an optical fiber [190] which can also have advanced imaging lenses [12] or manipulation tools attached to it [14], true *in situ* bioprinting inside a living human can be envisioned in the future. Finally, preclinical *in vivo* trials were also performed, showing that hard hybrid polymer 3D scaffolds can outperform standard collagen membranes in healing trauma [16]. The presented results were acquired in the time frame of up to 6 months. It proves that 3DLL made scaffolds can be implanted into living organisms for prolonged amount of times with the positive impact to the healing, which is the final goal of RM.

5. Challenges and Perspectives

The results presented so far show great potential of 3DLL in RM. Nevertheless, a lot more needs to be done before it becomes a widespread solution. Here, we look into some of the newest trends in 3DLL with the emphasis on how these can benefit RM in the future.

Biocompatibility is the key requirement in RM. While a lot of biocompatible materials were tested already [26, 124,

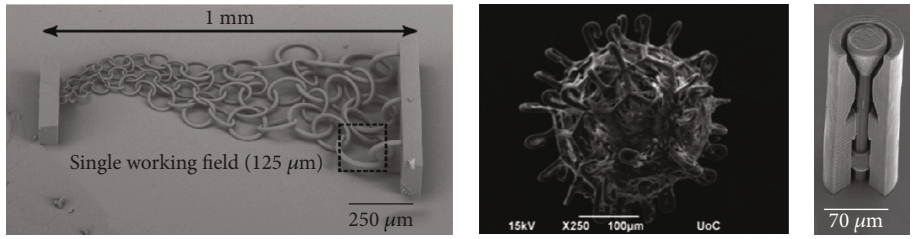

(a) (b) (c)

Figure 13: (a) A gradient chainmail-like structure which could be used as a mechanically flexible scaffold while still being made out of hard material. The mm scale size is sufficient for usage in real clinical trials. It is important to note that it was done using a galvo scanner and linear stage synchronization allowing to avoid stitching. It would have been detrimental to the mechanical quality of the structure (Adapted with permission from [6] © The Optical Society.). (b) Burr-like ball seeded with cells. Due to the geometry of the structure and hook-like outer ends, multiples of such objects can join together in the wound forming a shape-replicating structure (Reproduced from [113], with the permission of American Vacuum Society.). (c) Example of a passive microvalve allowing the flow of liquid only in one direction. Enhanced and custom-tuned objects of this kind could potentially be used in the veins to replace worn out biological analogs (adopted from [110]).

188], this area is still relatively active. The key questions here are compromise between effectiveness of PI and fabrication throughput, dissolvability in water, and other appropriate solvents and long-term effects of PI presence in the living body. Indeed, some materials require extensive exposure to fully start the polymerization reaction [52]. Fast-acting PIs are being constantly developed [191]. Thus, one might expect that with the constant increase in fabrication throughput photoexcitation should not become the bottleneck of the 3DLL. What is more, these fast-acting new generation PIs are also being made to be dissolvable in water, allowing them to be used in biodegradable hydrogels [151]. On the other hand, they also have to be biocompatible. Some of the long-term studies showed that in some cases, PI can be completely inert in nondegradable scaffolds even after being in a living organism for up to 6 months [16]. Hydrogel-compatible high-speed PIs also show great promise in this regard [151]. However, more research in this area is needed. Also, one must not forget about the possibility to directly polymerize materials without PI completely forgoing the problem of PI's biocompatibility [133, 154]. This is especially true keeping in mind that PI-free printing was shown to be applicable even at high-speed fabrication.

The next challenge lies in producing deformable scaffolds and structures that could move inside soft tissue after being implanted. Most 3DLL-processable materials are relatively stiff, with Young's modulus well into ~GPa. Therefore, bone tissue replacement is one of the main areas where 3DLL was tested extensively [16, 189]. In order to apply it for soft tissue, several 3DLL-enabled tricks were also employed. A scaffold can have deformable geometry due to being made out of intertwined parts [6] (Figure 13(a)) or having very small features that can deform [13, 14]. Also, shape-shifting scaffolds made out of microballs seeded with cells are also an interesting prospect [113] (Figure 13(b)). However, true 3D nanostructuring of elastomer is desired. Despite this, so far, it was shown to be relatively complicated for several reasons. If standard PDMS is used, translation velocity is limited and/or the fabrication window is narrow (in comparison to standard 3DLL materials) [121, 122]. Shrinkage can also be a problem [124]. Current progress in the field allows to relatively easily print mm scale scaffolds out of elastic materials [192]. Further downscaling could be expected in near future.

Alongside movement of soft tissue, mechanical flexibility is also relevant for mechanical metamaterials. In short, metamaterials are artificial materials with rationally designed features allowing properties beyond what is normally possible in nature [193], hence the Greek word *meta*, which means "beyond." So far, it was demonstrated that 3DLL is capable of producing objects with negative Poisson index [194], controllable thermal expansion [13], and negative effective static compressibility [195]. The prospect of such special properties on-demand brings the new dimension to RM. First, 3D microprinted stents become a possibility [196]. Then, basically any-sized blood vessel can be accommodated with them. Furthermore, scaffold reacting to the temperature, pressure, or chemical composition of surroundings can be created. Indeed, the polymer has an inherent property to swell or expand in the different liquids [197], meaning that the scaffold can react to this as well, potentially protecting cells from adverse materials in the immediate surrounding or, alternatively, opening more when special healing liquids are present. Overall, combining unlimited 3D geometry and smart architecture has a huge promise in RM, and one can expect this area to be exploited more and more in the near future.

Purpose-driven material development also led to polymers that can be dissolved after manufacturing. Indeed, 3DLL supports multimaterial printing [17, 197–199]. While it is already a powerful tool in RM, the possibility to "erase" some of the components that were 3D printed is an interesting prospect. Thus, polymers based and dissolvable in softer chemical solutions were developed [200]. The implication to RM is scaffolds that can be dissolved in the body at different stages on the treatment. Furthermore, keeping in mind diverse chemistry of the body, such scaffolds might be degraded by the body itself. Also, nondegradable and permanent materials might be combined in one structure. One of the possible applications could be a nondegradable valve [110] (Figure 13(c)) placed in veins with accompanying scaffold for better initial growth. After some time, the

scaffold would degrade leaving a very well-attached permanent valve.

Finally, material development should not overshadow challenges in the hardware and software needed for 3DLL. The key advances here are related to minimized workload to the user and increased throughput. Operator workload is being reduced by employing advanced software, which allows to perform monotonous tasks (for instance, structure placement on substrate) and printing optimization easier [70, 74]. In terms of hardware, additional components can be placed into the optical path enhancing throughout or versatility of the setup. The primary example in this regard is the spatial light modulator (SLM), which might help to increase fabrication throughput [201, 202]. If a cheaper and simpler solution is required, passive light shaping can be done [203, 204] sacrificing flexibility and tunability. Spatiotemporal light shaping is also possible [62, 63]. While it is highly promising for RM due to the capability to print relatively big (up to cm) structures, it has a disadvantage of being relatively complicated. Lastly, hardware solutions for very fast translation velocities are also coming. Current positioning systems based on galvo scanners, linear stages, or their synchronization can go as fast as mm/s–cm/s [6, 72]. However, with the advent of polygon scanners [205] and acoustooptics [206], these translation velocities might exceed m/s or even more. Nevertheless, both of these solutions have some distinct limitations. Polygon scanners cannot easily change the direction of scanning and have limited flexibility. Thus, they are suitable only for mass production of designs that will not change or will change minimally. Acoustooptical deflectors do not have this problem but are bound by limitation in sustaining polarization and possible temporal broadening of a fs pulse due to the severe dispersion. Therefore, a lot of work has to be done in order to apply these solutions to 3DLL technology.

6. Conclusions

RM is an extremely complex and challenging topic. As shown in this review, 3DLL is capable of overcoming these challenges. One of the main reasons is the extremely wide selection of materials and structuring regimes. Indeed, combining free choice of 3D architecture of a structure and usage-specific monomer-PI covers basically any need for RM, starting from hard scaffolds for bone regeneration to EM-imitating multicomponent structures. Keeping in mind that new materials directly tailored for this field are being constantly developed, printing technology improved, and new 3D geometries tested, one might realistically expect widespread adoption of this technology in the near future.

Conflicts of Interest

The authors declare that they have no conflicts of interest.

Authors' Contributions

G.M. prepared information concerning the materials discussed in the article. L.J. contributed parts discussing the technology and trends in the field. D.G. and S.S. provided general insights. All authors contributed to the preparation of the manuscript.

Acknowledgments

The Lithuanian Business Support Agency project no. J05-LVPA-K-03-0006 is acknowledged for financial support.

References

[1] L. Jonušauskas, S. Juodkazis, and M. Malinauskas, "Optical 3D printing: bridging the gaps in the mesoscale," *Journal of Optics*, vol. 20, article 053001, 2018.

[2] M. Malinauskas, A. Žukauskas, G. Bičkauskaitė, R. Gadonas, and S. Juodkazis, "Mechanisms of three-dimensional structuring of photo-polymers by tightly focussed femtosecond laser pulses," *Optics Express*, vol. 18, pp. 10209–10221, 2010.

[3] W. Haske, V. W. Chen, J. M. Hales et al., "65 nm feature sizes using visible wavelength 3-D multiphoton lithography," *Optics Express*, vol. 15, no. 6, pp. 3426–3436, 2007.

[4] M. Emons, K. Obata, T. Binhammer, A. Ovsianikov, B. N. Chichkov, and U. Morgner, "Two-photon polymerization technique with sub-50 nm resolution by sub-10 fs laser pulses," *Optical Materials Express*, vol. 2, no. 7, pp. 942–947, 2012.

[5] L. Jonušauskas, S. Rekštyte, R. Buividas et al., "Hybrid subtractive-additive-welding microfabrication for lab-on-chip (LOC) applications via single amplified femtosecond laser source," *Optical Engineering*, vol. 56, article 094108, 2017.

[6] L. Jonušauskas, D. Gailevičius, S. Rekštytė, T. Baldacchini, S. Juodkazis, and M. Malinauskas, "Mesoscale laser 3D printing," *Optics Express*, vol. 27, no. 11, pp. 15205–15221, 2019.

[7] M. Farsari, M. Vamvakaki, and B. N. Chichkov, "Multiphoton polymerization of hybrid materials," *Journal of Optics*, vol. 12, no. 12, p. 124001, 2010.

[8] C. Barner-Kowollik, M. Bastmeyer, E. Blasco et al., "3D Laser Micro- and Nanoprinting: Challenges for Chemistry," *Angewandte Chemie, International Edition*, vol. 56, no. 50, pp. 15828–15845, 2017.

[9] L. Maigyte, V. Purlys, J. Trull et al., "Flat lensing in the visible frequency range by woodpile photonic crystals," *Optics Letters*, vol. 38, no. 14, pp. 2376–2378, 2013.

[10] A. I. Aristov, M. Manousidaki, A. Danilov et al., "3D plasmonic crystal metamaterials for ultra-sensitive biosensing," *Scientific Reports*, vol. 6, no. 1, article 25380, 2016.

[11] C. Liberale, G. Cojoc, F. Bragheri et al., "Integrated microfluidic device for single-cell trapping and spectroscopy," *Scientific Reports*, vol. 3, no. 1, p. 1258, 2013.

[12] T. Gissibl, S. Thiele, A. Herkommer, and H. Giessen, "Two-photon direct laser writing of ultracompact multi-lens objectives," *Nature Photonics*, vol. 10, no. 8, pp. 554–560, 2016.

[13] J. Qu, M. Kadic, A. Naber, and M. Wegener, "Micro-structured two-component 3d metamaterials with negative thermal-expansion coefficient from positive constituents," *Scientific Reports*, vol. 7, no. 1, article 40643, 2017.

[14] M. Power, A. J. Thompson, S. Anastasova, and G.-Z. Yang, "A monolithic force-sensitive 3D microgripper fabricated on the tip of an optical fiber using 2-photon polymerization," *Small*, vol. 14, no. 16, article 1703964, 2018.

[15] D. Wu, S. Z. Wu, J. Xu, L. G. Niu, K. Midorikawa, and K. Sugioka, "Hybrid femtosecond laser microfabrication to achieve true 3D glass/polymer composite biochips with multiscale features and high performance: the concept of ship-in-a-bottle biochip," *Laser & Photonics Reviews*, vol. 8, no. 3, pp. 458–467, 2014.

[16] J. Mačiulaitis, M. Deveikytė, S. Rekštytė et al., "Preclinical study of SZ2080 material 3D microstructured scaffolds for cartilage tissue engineering made by femtosecond direct laser writing lithography," *Biofabrication*, vol. 7, no. 1, article 015015, 2015.

[17] B. Richter, V. Hahn, S. Bertels et al., "Guiding cell attachment in 3D microscaffolds selectively functionalized with two distinct adhesion proteins," *Advanced Materials*, vol. 29, no. 5, article 1604342, 2017.

[18] S. Maruo, O. Nakamura, and S. Kawata, "Three-dimensional microfabrication with two-photon-absorbed photopolymerization," *Optics Letters*, vol. 22, no. 2, pp. 132–134, 1997.

[19] Z.-J. Chen, J. Yao, Q.-J. Xu, and Z.-H. Wang, "Two-photon polymerization fabrication and Raman spectroscopy research of SU-8 photoresist using the femtosecond laser," *Optoelectronics Letters*, vol. 13, no. 3, pp. 210–213, 2017.

[20] A. Ovsianikov, M. Gruene, M. Pflaum et al., "Laser printing of cells into 3D scaffolds," *Biofabrication*, vol. 2, no. 1, article 014104, 2010.

[21] J. Serbin, A. Egbert, A. Ostendorf et al., "Femtosecond laser-induced two-photon polymerization of inorganic-organic hybrid materials for applications in photonics," *Optics Letters*, vol. 28, no. 5, pp. 301–303, 2003.

[22] D. S. Correa, P. Tayalia, G. Cosendey et al., "Two-photon polymerization for fabricating structures containing the biopolymer chitosan," *Journal of Nanoscience and Nanotechnology*, vol. 9, no. 10, pp. 5845–5849, 2009.

[23] C. Mason and P. Dunnill, "A brief definition of regenerative medicine," *Regenerative Medicine*, vol. 3, no. 1, pp. 1–5, 2008.

[24] R. J. Narayan, A. Doraiswamy, D. B. Chrisey, and B. N. Chichkov, "Medical prototyping using two photon polymerization," *Materials Today*, vol. 13, no. 12, pp. 42–48, 2010.

[25] M. T. Raimond, S. M. Eaton, M. M. Nava, M. Laganà, G. Cerullo, and R. Osellame, "Two-photon laser polymerization: from fundamentals to biomedical application in tissue engineering and regenerative medicine," *Journal of Applied Biomaterials & Functional Materials*, vol. 10, no. 1, pp. 56–66, 2012.

[26] J. Torgersen, X. H. Qin, Z. Li, A. Ovsianikov, R. Liska, and J. Stampfl, "Hydrogels for Two-Photon Polymerization: A Toolbox for Mimicking the Extracellular Matrix," *Advanced Functional Materials*, vol. 23, no. 36, pp. 4542–4554, 2013.

[27] T. Stichel, B. Hecht, R. Houbertz, and G. Sextl, "Two-photon polymerization as method for the fabrication of large scale biomedical scaffold applications," *Journal of Laser Micro/Nanoengineering*, vol. 5, no. 3, pp. 209–212, 2010.

[28] A. Trautmann, M. Ruth, H.-D. Lemke, T. Walther, and R. Hellmann, "Two-photon polymerization based large scaffolds for adhesion and proliferation studies of human primary fibroblasts," *Optics & Laser Technology*, vol. 106, pp. 474–480, 2018.

[29] B.-B. Xu, Y. L. Zhang, H. Xia, W. F. Dong, H. Ding, and H. B. Sun, "Fabrication and multifunction integration of microfluidic chips by femtosecond laser direct writing," *Lab on a Chip*, vol. 13, no. 9, pp. 1677–1690, 2013.

[30] S. D. Gittard, A. Ovsianikov, B. N. Chichkov, A. Doraiswamy, and R. J. Narayan, "Two-photon polymerization of microneedles for transdermal drug delivery," *Expert Opinion on Drug Delivery*, vol. 7, no. 4, pp. 513–533, 2010.

[31] C.-H. Lin, G.-B. Lee, B.-W. Chang, and G.-L. Chang, "A new fabrication process for ultra-thick microfluidic microstructures utilizing SU-8 photoresist," *Journal of Micromechanics and Microengineering*, vol. 12, no. 5, pp. 590–597, 2002.

[32] D. T. Pham, S. S. Dimov, and R. S. Gault, "Part orientation in stereolithography," *International Journal of Advanced Manufacturing Technology*, vol. 15, no. 9, pp. 674–682, 1999.

[33] M. Han, W. Lee, S.-K. Lee, and S. S. Lee, "3D microfabrication with inclined/rotated UV lithography," *Sensors and Actuators A: Physical*, vol. 111, no. 1, pp. 14–20, 2004.

[34] G. Grigalevičiūtė, D. Baltriukienė, E. Balčiūnas, L. Jonušauskas, and M. Malinauskas, "Fabrication of flexible microporous 3D scaffolds via stereolithography and optimization of their biocompatibility," in *Advanced Fabrication Technologies for Micro/Nano Optics and Photonics XI*, vol. 10544, San Francisco, CA, USA, 2018.

[35] M. Göppert-Mayer, "Über elementarakte mit zwei quantensprüngen," *Annalen der Physik*, vol. 401, pp. 273–294, 1931.

[36] W. Kaiser and C. G. B. Garrett, "Two-photon excitation in CaF_2:Eu^{2+}," *Physical Review Letters*, vol. 7, pp. 229–231, 1961.

[37] R. R. Birge and B. M. Pierce, "Semiclassical time-dependent theory of two-photon spectroscopy. The effect of dephasing in the virtual level on the two-photon excitation spectrum of isotachysterol," *International Journal of Quantum Chemistry*, vol. 29, pp. 639–656, 1986.

[38] M. Farsari, G. Filippidis, and C. Fotakis, "Fabrication of three-dimensional structures by three-photon polymerization," *Optics Letters*, vol. 30, no. 23, pp. 3180–3182, 2005.

[39] J. Fischer, J. B. Mueller, J. Kaschke, T. J. A. Wolf, A. N. Unterreiner, and M. Wegener, "Three-dimensional multi-photon direct laser writing with variable repetition rate," *Optics Express*, vol. 21, no. 22, pp. 26244–26260, 2013.

[40] R. Buividas, S. Rekštyte, M. Malinauskas, and S. Juodkazis, "Nano-groove and 3D fabrication by controlled avalanche using femtosecond laser pulses," *Optical Materials Express*, vol. 3, no. 10, pp. 1674–1686, 2013.

[41] K. K. Seet, S. Juodkazis, V. Jarutis, and H. Misawa, "Feature-size reduction of photopolymerized structures by femtosecond optical curing of SU-8," *Applied Physics Letters*, vol. 89, no. 2, article 024106, 2006.

[42] M. Thiel, J. Fischer, G. Freymann, and M. Wegener, "Direct laser writing of three-dimensional submicron structures using a continuous-wave laser at 532 nm," *Applied Physics Letters*, vol. 97, no. 22, article 221102, 2010.

[43] A. I. Ciuciu and P. J. Cywinski, "Two-photon polymerization of hydrogels – versatile solutions to fabricate well-defined 3D structures," *RSC Advances*, vol. 4, no. 85, pp. 45504–45516, 2014.

[44] J. Fouassier, *Photoinitiation Photopolymerization and Photocuring*, Hanser Publishers, 1995.

[45] K. Haraguchi and T. Takehisa, "Nanocomposite hydrogels: a unique organic-inorganic network structure with extraordinary mechanical, optical, and swelling/de-swelling properties," *Advanced Materials*, vol. 14, pp. 1120–1124, 2002.

[46] S. Edmondson and M. Gilbert, "Chapter 2 - the chemical nature of plastics polymerization," in *Brydson's Plastics*

Materials (Eighth Edition), M. Gilbert, Ed., pp. 19–37, Butterworth-Heinemann, 2017.

[47] W.-F. Su, "Radical Chain Polymerization," in *Principles of Polymerization*, pp. 198–349, Springer, Berlin Heidelberg, Berlin, Heidelberg, 2013.

[48] J. Kreutzer and Y. Yagci, "Metal free reversible-deactivation radical polymerizations: advances, challenges, and opportunities," *Polymers*, vol. 10, no. 1, p. 35, 2017.

[49] N. Alharbi, R. Osman, and D. Wismeijer, "Effects of build direction on the mechanical properties of 3D-printed complete coverage interim dental restorations," *The Journal of Prosthetic Dentistry*, vol. 115, no. 6, pp. 760–767, 2016.

[50] J. V. Crivello, *Polymer Science: A Comprehensive Reference, vol. 4*, Elsevier Science, 2012.

[51] K. T. Nguyen and J. L. West, "Photopolymerizable hydrogels for tissue engineering applications," *Biomaterials*, vol. 23, no. 22, pp. 4307–4314, 2002.

[52] E. Skliutas, S. Kašetaite, L. Jonušauskas, J. Ostrauskaite, and M. Malinauskas, "Photosensitive naturally derived resins toward optical 3-D printing," *Optical Engineering*, vol. 57, no. 4, p. 1, 2018.

[53] I. Sakellari, E. Kabouraki, D. Gray et al., "Diffusion-assisted high-resolution direct femtosecond laser writing," *ACS Nano*, vol. 6, no. 3, pp. 2302–2311, 2012.

[54] P. Prabhakaran, Y. Son, C. W. Ha, J. J. Park, S. Jeon, and K. S. Lee, "Optical materials forming tightly polymerized voxels during laser direct writing," *Advanced Engineering Materials*, vol. 20, no. 10, article 1800320, 2018.

[55] A. Žukauskas, I. Matulaitienė, D. Paipulas, G. Niaura, M. Malinauskas, and R. Gadonas, "Tuning the refractive index in 3D direct laser writing lithography: towards GRIN microoptics," *Laser & Photonics Reviews*, vol. 9, no. 6, pp. 706–712, 2015.

[56] M. Malinauskas, G. Bičkauskaitė, M. Rutkauskas, D. Paipulas, V. Purlys, and R. Gadonas, "Self-polymerization of nanofibres and nano-membranes induced by two-photon absorption," *Lithuanian Journal of Physics*, vol. 50, no. 1, pp. 135–140, 2010.

[57] M. Gernhardt, E. Blasco, M. Hippler et al., "Tailoring the mechanical properties of 3d microstructures using visible light post-manufacturing," *Advanced Materials*, vol. 31, article 1901269, 2019.

[58] L. Jonušauskas, D. Mackevičiūtė, G. Kontenis, and V. Purlys, "Femtosecond lasers: the ultimate tool for high-precision 3D manufacturing," *Advanced Optical Technologies*, vol. 8, no. 3-4, pp. 241–251, 2019.

[59] M. Malinauskas, P. Danilevicius, and S. Juodkazis, "Three-dimensional micro-/nano-structuring via direct write polymerization with picosecond laser pulses," *Optics Express*, vol. 19, no. 6, pp. 5602–5610, 2011.

[60] E. Stankevicius, E. Daugnoraite, A. Selskis, S. Juodkazis, and G. Račiukaitis, "Photo-polymerization differences by using nanosecond and picosecond laser pulses," *Optics Express*, vol. 25, no. 5, pp. 4819–4830, 2017.

[61] T. Tičkūnas, M. Perrenoud, S. Butkus et al., "Combination of additive and subtractive laser 3D microprocessing in hybrid glass/polymer microsystems for chemical sensing applications," *Optics Express*, vol. 25, no. 21, pp. 26280–26288, 2017.

[62] F. He, H. Xu, Y. Cheng et al., "Fabrication of microfluidic channels with a circular cross section using spatiotemporally focused femtosecond laser pulses," *Optics Letters*, vol. 35, no. 7, pp. 1106–1108, 2010.

[63] Y. Tan, W. Chu, P. Wang et al., "High-throughput multi-resolution three dimensional laser printing," *Physica Scripta*, vol. 94, no. 1, article 015501, 2018.

[64] J. Hering, E. H. Waller, and G. Von Freymann, "Automated aberration correction of arbitrary laser modes in high numerical aperture systems," *Optics Express*, vol. 24, no. 25, pp. 28500–28508, 2016.

[65] M. Straub and M. Gu, "Near-infrared photonic crystals with higher-order bandgaps generated by two-photon photopolymerization," *Optics Letters*, vol. 27, no. 20, pp. 1824–1826, 2002.

[66] K. Obata, A. El-Tamer, L. Koch, U. Hinze, and B. N. Chichkov, "High-aspect 3D two-photon polymerization structuring with widened objective working range (WOW-2PP)," *Light: Science & Applications*, vol. 2, no. 12, article e116, 2013.

[67] J. S. Oakdale, R. F. Smith, J. B. Forien et al., "*Direct Laser Writing of Low-Density Interdigitated Foams for Plasma Drive Shaping*," *Advanced Functional Materials*, vol. 27, no. 43, article 1702425, 2017.

[68] J. Li, P. Fejes, D. Lorenser et al., "Two-photon polymerisation 3D printed freeform micro-optics for optical coherence tomography fibre probes," *Scientific Reports*, vol. 8, no. 1, p. 14789, 2018.

[69] H. Ni, G. Yuan, L. Sun et al., "Large-scale high-numerical-aperture super-oscillatory lens fabricated by direct laser writing lithography," *RSC Advances*, vol. 8, no. 36, pp. 20117–20123, 2018.

[70] S. Dehaeck, B. Scheid, and P. Lambert, "Adaptive stitching for meso-scale printing with two-photon lithography," *Additive Manufacturing*, vol. 21, pp. 589–597, 2018.

[71] P. Danilevičius, S. Rekštytė, E. Balčiūnas et al., "Direct laser fabrication of polymeric implants for cardiovascular surgery," *Materials Science*, vol. 18, pp. 145–149, 2012.

[72] J. Torgersen, A. Ovsianikov, V. Mironov et al., "Photo-sensitive hydrogels for three-dimensional laser microfabrication in the presence of whole organisms," *Journal of Biomedical Optics*, vol. 17, no. 10, article 105008, 2012.

[73] D. Ricci, M. Nava, T. Zandrini, G. Cerullo, M. Raimondi, and R. Osellame, "Scaling-up techniques for the nanofabrication of cell culture substrates via two-photon polymerization for industrial-scale expansion of stem cells," *Materials*, vol. 10, no. 1, p. 66, 2017.

[74] E. Yulianto, S. Chatterjee, V. Purlys, and V. Mizeikis, "Imaging of latent three-dimensional exposure patterns created by direct laser writing in photoresists," *Applied Surface Science*, vol. 479, pp. 822–827, 2019.

[75] M. Manousidaki, D. G. Papazoglou, M. Farsari, and S. Tzortzakis, "Abruptly autofocusing beams enable advanced multiscale photo-polymerization," *Optica*, vol. 3, no. 5, pp. 525–530, 2016.

[76] Y. Y. Schechner, N. Kiryati, and J. Shamir, "Separation of transparent layers by polarization analysis," *Surfaces*, vol. 8, p. 18, 1999.

[77] C. N. LaFratta and T. Baldacchini, "Two-photon polymerization metrology: characterization methods of mechanisms and microstructures," *Micromachines*, vol. 8, no. 4, p. 101, 2017.

[78] V. R. Sastri, "Chapter 7 - Engineering thermoplastics: acrylics, polycarbonates, polyurethanes, polyacetals, polyesters, and

polyamides," in *Plastics in Medical Devices*, pp. 121–173, William Andrew, 2010.

[79] S. Sarkar, K. B. Visscher, D. K. Hood, and C. J. Wasserman, "National Center for Biotechnology Information," Patent US2016282737, 2014.

[80] U. Ali, K. J. Abd Karim, and N. Buang, "A review of the properties and applications of poly (methyl methacrylate) (pmma)," *Polymer Reviews*, vol. 55, no. 4, pp. 678–705, 2015.

[81] M. Rahmah, N. Razali, A. Ehsan, and S. Shaari, "Characterisation and process optimisation of photosensitive acrylates for photonics applications," *Science and Technology of Advanced Materials*, vol. 6, no. 3-4, pp. 375–382, 2005.

[82] T. Baldacchini, C. N. LaFratta, R. A. Farrer et al., "Acrylic-based resin with favorable properties for three-dimensional two-photon polymerization," *Journal of Applied Physics*, vol. 95, no. 11, pp. 6072–6076, 2004.

[83] M. Farsari, G. Filippidis, K. Sambani, T. S. Drakakis, and C. Fotakis, "Two-photon polymerization of an eosin Y-sensitized acrylate composite," *Journal of Photochemistry and Photobiology A: Chemistry*, vol. 181, no. 1, pp. 132–135, 2006.

[84] R. J. Winfield and S. O'Brien, "Two-photon polymerization of an epoxy-acrylate resin material system," *Applied Surface Science*, vol. 257, no. 12, pp. 5389–5392, 2011.

[85] T. Zandrini, N. Liaros, L. J. Jiang et al., "Effect of the resin viscosity on the writing properties of two-photon polymerization," *Optical Materials Express*, vol. 9, no. 6, pp. 2601–2616, 2019.

[86] A. Campo and C. Greiner, "SU-8: a photoresist for high-aspect-ratio and 3D submicron lithography," *Journal of Micromechanics and Microengineering*, vol. 17, no. 6, pp. R81–R95, 2007.

[87] G. Witzgall, R. Vrijen, E. Yablonovitch, V. Doan, and B. J. Schwartz, "Single-shot two-photon exposure of commercial photoresist for the production of three-dimensional structures," *Optics Letters*, vol. 23, no. 22, pp. 1745–1747, 1998.

[88] W. H. Teh, U. Dürig, G. Salis et al., "SU-8 for real three-dimensional subdiffraction-limit two-photon microfabrication," *Applied Physics Letters*, vol. 84, no. 20, pp. 4095–4097, 2004.

[89] B. Bilenberg, S. Jacobsen, M. S. Schmidt et al., "High resolution 100 kV electron beam lithography in SU-8," *Microelectronic Engineering*, vol. 83, no. 4-9, pp. 1609–1612, 2006.

[90] Y. Liu, D. D. Nolte, and L. J. Pyrak-Nolte, "Large-format fabrication by two-photon polymerization in SU-8," *Applied Physics A: Materials Science & Processing*, vol. 100, no. 1, pp. 181–191, 2010.

[91] H. E. Williams, D. J. Freppon, S. M. Kuebler, R. C. Rumpf, and M. A. Melino, "Fabrication of three-dimensional micro-photonic structures on the tip of optical fibers using SU-8," *Optics Express*, vol. 19, no. 23, pp. 22910–22922, 2011.

[92] J. Serbin, A. Ovsianikov, and B. Chichkov, "Fabrication of woodpile structures by two-photon polymerization and investigation of their optical properties," *Optics Express*, vol. 12, no. 21, pp. 5221–5228, 2004.

[93] M. F. Akhtar, M. Hanif, and N. M. Ranjha, "Methods of synthesis of hydrogels … A review," *Saudi Pharmaceutical Journal*, vol. 24, no. 5, pp. 554–559, 2016.

[94] E. Ahmed and M. Hydrogel, "Hydrogel: Preparation, characterization, and applications: A review," *Journal of Advanced Research*, vol. 6, no. 2, pp. 105–121, 2015.

[95] A. Ovsianikov, M. Malinauskas, S. Schlie et al., "Three-dimensional laser micro- and nano-structuring of acrylated poly(ethylene glycol) materials and evaluation of their cytoxicity for tissue engineering applications," *Acta Biomaterialia*, vol. 7, no. 3, pp. 967–974, 2010.

[96] L. D. V. Lith, *Functionalization of Poly-(Ethylene Glycol)-Diacrylate (PEGda) with Different Molecular Mass using Two-Photon-Polymerisation*, TU Dresden, 2016.

[97] O. Kufelt, A. el-Tamer, C. Sehring, M. Meißner, S. Schlie-Wolter, and B. N. Chichkov, "Water-soluble photopolymerizable chitosan hydrogels for biofabrication via two-photon polymerization," *Acta Biomaterialia*, vol. 18, pp. 186–195, 2015.

[98] J.-F. Xing, M.-L. Zheng, and X.-M. Duan, "Two-photon polymerization microfabrication of hydrogels: an advanced 3D printing technology for tissue engineering and drug delivery," *Chemical Society Reviews*, vol. 44, no. 15, pp. 5031–5039, 2015.

[99] A. Dehghan and J. Ansary, "Sol-gel process applications: a mini-review," *Proceedings of the Nature Research Society*, vol. 2, article 02008, 2018.

[100] J. Livage, "Sol-gel processes," *Current Opinion in Solid State & Materials Science*, vol. 2, no. 2, pp. 132–138, 1997.

[101] R. D. Maggio, S. Dirè, E. Callone, F. Girardi, and G. Kickelbick, "Hybrid organic-inorganic materials using zirconium based NBBs and vinyl trimethoxysilane: Effect of prehydrolysis of silane," *Polymer*, vol. 51, no. 4, pp. 832–841, 2010.

[102] F. Osterholtz and E. Pohl, "Kinetics of the hydrolysis and condensation of organofunctional alkoxysilanes: a review," *Journal of Adhesion Science and Technology*, vol. 6, no. 1, pp. 127–149, 1992.

[103] C. Michelina and F. Bollino, "Synthesis and characterization of amorphous and hybrid materials obtained by sol-gel processing for biomedical applications," in *Biomedical Science, Engineering and Technology*, D. N. Ghista, Ed., IntechOpen, 2012.

[104] B. Arkles, J. Steinmetz, J. Zazyczny, and P. Mehta, "Factors contributing to the stability of alkoxysilanes in aqueous solution," *Journal of Adhesion Science and Technology*, vol. 6, no. 1, pp. 193–206, 1992.

[105] C. Brinker, "Hydrolysis and condensation of silicates: effects on structure," *Journal of Non-Crystalline Solids*, vol. 100, no. 1-3, pp. 31–50, 1988.

[106] A. Ovsianikov, J. Viertl, B. Chichkov et al., "Ultra-low shrinkage hybrid photosensitive material for two-photon polymerization microfabrication," *ACS Nano*, vol. 2, no. 11, pp. 2257–2262, 2008.

[107] M. Malinauskas, A. Žukauskas, V. Purlys et al., "3D microoptical elements formed in a photostructurable germanium silicate by direct laser writing," *Optics and Lasers in Engineering*, vol. 50, no. 12, pp. 1785–1788, 2012.

[108] I. Sakellari, A. Gaidukeviciute, A. Giakoumaki et al., "Two-photon polymerization of titanium-containing sol–gel composites for three-dimensional structure fabrication," *Applied Physics A: Materials Science & Processing*, vol. 100, no. 2, pp. 359–364, 2010.

[109] M. Malinauskas, A. Žukauskas, K. Belazaras et al., "Laser fabrication of various polymer microoptical components," *The European Physical Journal Applied Physics*, vol. 58, no. 2, article 20501, 2012.

[110] C. Schizas, V. Melissinaki, A. Gaidukeviciute et al., "On the design and fabrication by two-photon polymerization of a readily assembled micro-valve," *International Journal of Advanced Manufacturing Technology*, vol. 48, no. 5-8, pp. 435–441, 2010.

[111] A. Žukauskas, M. Malinauskas, L. Kontenis et al., "Organic dye doped microstructures for optically active functional devices fabricated via two-photon polymerization technique," *Lithuanian Journal of Physics*, vol. 50, no. 1, pp. 55–61, 2010.

[112] L. Jonušauskas, M. Lau, P. Gruber et al., "Plasmon assisted 3D microstructuring of gold nanoparticle-doped polymers," *Nanotechnology*, vol. 27, no. 15, article 154001, 2016.

[113] P. Danilevicius, R. A. Rezende, F. D. A. S. Pereira et al., "Burr-like, laser-made 3D microscaffolds for tissue spheroid encagement," *Biointerphases*, vol. 10, no. 2, article 021011, 2015.

[114] Y. Xia and G. M. Whitesides, "Soft lithography," *Annual Review of Materials Science*, vol. 28, no. 1, pp. 153–184, 1998.

[115] G. M. Whitesides, "The origins and the future of microfluidics," *Nature*, vol. 442, no. 7101, pp. 368–373, 2006.

[116] S. Baudis, B. Steyrer, T. Pulka et al., "Photopolymerizable elastomers for vascular tissue regeneration," *Macromolecular Symposia*, vol. 296, no. 1, pp. 121–126, 2010.

[117] K. Yu, A. Xin, H. Du, Y. Li, and Q. Wang, "Additive manufacturing of self-healing elastomers," *NPG Asia Materials*, vol. 11, pp. 1–11, 2019.

[118] E. Briganti, D. Spiller, C. Mirtelli et al., "A composite fibrin-based scaffold for controlled delivery of bioactive pro-angiogenetic growth factors," *Journal of Controlled Release*, vol. 142, pp. 14–21, 2010.

[119] A. D. Lantada, H. A. Iniesta, B. P. Sánchez, and J. P. García-Ruíz, "Free-form rapid prototyped porous PDMS scaffolds incorporating growth factors promote chondrogenesis," *Advances in Materials Science and Engineering*, vol. 2014, Article ID 612976, 10 pages, 2014.

[120] D. Martella and C. Parmeggiani, "Advances in cell scaffolds for tissue engineering: the value of liquid crystalline elastomers," *Chemistry - A European Journal*, vol. 24, pp. 12206–12220, 2018.

[121] C. A. Coenjarts and C. K. Ober, "Two-photon three-dimensional microfabrication of poly(dimethylsiloxane) elastomers," *Chemistry of Materials*, vol. 16, no. 26, pp. 5556–5558, 2004.

[122] H. Zeng, D. Martella, P. Wasylczyk et al., "High-Resolution 3D Direct Laser Writing for Liquid-Crystalline Elastomer Microstructures," *Advanced Materials*, vol. 26, no. 15, pp. 2319–2322, 2014.

[123] S. Rekštyte, M. Malinauskas, and S. Juodkazis, "Three-dimensional laser micro-sculpturing of silicone: towards biocompatible scaffolds," *Optics Express*, vol. 21, no. 14, pp. 17028–17041, 2013.

[124] S. Pashneh-Tala, R. Owen, H. Bahmaee, S. Rekštytė, M. Malinauskas, and F. Claeyssens, "Synthesis, characterization and 3D micro-structuring via 2-photon polymerization of poly(glycerol sebacate)-methacrylate - an elastomeric degradable polymer," *Frontiers of Physics*, vol. 6, p. 41, 2018.

[125] T. Ohkita and S.-H. Lee, "Thermal degradation and biodegradability of poly (lactic acid)/corn starch biocomposites," *Journal of Applied Polymer Science*, vol. 100, no. 4, pp. 3009–3017, 2006.

[126] L. Jonušauskas, E. Skliutas, S. Butkus, and M. Malinauskas, "Custom on demand 3D printing of functional microstructures," *Lithuanian Journal of Physics*, vol. 55, no. 3, pp. 227–236, 2015.

[127] J. Torres, J. Cotelo, J. Karl, and A. P. Gordon, "Mechanical property optimization of FDM PLA in shear with multiple objectives," *JOM*, vol. 67, no. 5, pp. 1183–1193, 2015.

[128] E. Garskaite, L. Alinauskas, M. Drienovsky et al., "Fabrication of a composite of nanocrystalline carbonated hydroxyapatite (cHAP) with polylactic acid (PLA) and its surface topographical structuring with direct laser writing (DLW)," *RSC Advances*, vol. 6, no. 76, pp. 72733–72743, 2016.

[129] M. Lebedevaite, J. Ostrauskaite, E. Skliutas, and M. Malinauskas, "Photoinitiator free resins composed of plant-derived monomers for the optical μ-3D printing of thermosets," *Polymers*, vol. 11, p. 116, 2019.

[130] K. Maximova, X. Wang, A. Balčytis, L. Fan, J. Li, and S. Juodkazis, "Silk patterns made by direct femtosecond laser writing," *Biomicrofluidics*, vol. 10, no. 5, article 054101, 2016.

[131] Y.-L. Sun, Q. Li, S. M. Sun et al., "Aqueous multiphoton lithography with multifunctional silk-centred bio-resists," *Nature Communications*, vol. 6, no. 1, pp. 1–10, 2015.

[132] S. J. J. Kwok, I. A. Kuznetsov, M. Kim, M. Choi, G. Scarcelli, and S. H. Yun, "Selective two-photon collagen crosslinking *in situ* measured by Brillouin microscopy," *Optica*, vol. 3, no. 5, pp. 469–472, 2016.

[133] K. Parkatzidis, E. Kabouraki, A. Selimis et al., "Initiator-Free, Multiphoton Polymerization of Gelatin Methacrylamide," *Macromolecular Materials and Engineering*, vol. 303, no. 12, article 1800458, 2018.

[134] M. Shirai and H. Okamura, "UV-curable positive photoresists for screen printing plate," *Polymer International*, vol. 65, no. 4, pp. 362–370, 2016.

[135] X. Zheng, C. Ji, Q. Zeng et al., "Synthesis of novel copolymer based on precipitation polymerization and its application in positive-tone photoresist," *Journal of Polymer Research*, vol. 24, no. 11, article 1370, 2017.

[136] N. Tsutsumi, A. Fukuda, R. Nakamura, K. Kinashi, and W. Sakai, "Fabrication of three-dimensional microstructures in positive photoresist through two-photon direct laser writing," *Applied Physics A*, vol. 123, no. 8, p. 553, 2017.

[137] H.-Z. Cao, M.-L. Zheng, X.-Z. Dong, F. Jin, Z.-S. Zhao, and X.-M. Duan, "Two-photon nanolithography of positive photoresist thin film with ultrafast laser direct writing," *Applied Physics Letters*, vol. 102, no. 20, article 201108, 2013.

[138] O. Wei, F. Hu, and L. Wang, "Formation of nanotunnels inside a resist film in laser interference lithography," *Langmuir*, vol. 31, no. 19, pp. 5464–5468, 2015.

[139] S. Z. Huang and K. Y. Wu, "Health risk assessment of photoresists used in an optoelectronic semiconductor factory," *Risk Analysis*, 2019.

[140] A. Soyano, "Application of polymers to photoresist materials," *International Polymer Science and Technology*, vol. 39, pp. 47–54, 2012.

[141] W. Zhou, S. M. Kuebler, K. L. Braun et al., "An efficient two-photon-generated photoacid applied to positive-tone 3D microfabrication," *Science*, vol. 296, no. 5570, pp. 1106–1109, 2002.

[142] T. Yu, C. K. Ober, S. M. Kuebler, W. Zhou, S. R. Marder, and J. W. Perry, "Chemically amplified positive resists for two-

photon three-dimensional microfabrication," *Advanced Materials*, vol. 15, no. 6, pp. 517–521, 2003.

[143] S. M. Kuebler, K. L. Braun, W. Zhou et al., "Design and application of high-sensitivity two-photon initiators for three-dimensional microfabrication," *Journal of Photochemistry and Photobiology A: Chemistry*, vol. 158, no. 2-3, pp. 163–170, 2003.

[144] B. D. Zhao, G. L. Li, Y. Z. Shi, H. Q. Zhang, and T. Wang, "Synthesis and optical properties of novel d-π-a-π-d type cationic cyclopentadienyliron complexes of arenes," *RSC Advances*, vol. 5, no. 67, pp. 54749–54756, 2015.

[145] Z. Li, J. Torgersen, A. Ajami et al., "Initiation efficiency and cytotoxicity of novel water-soluble two-photon photoinitiators for direct 3d microfabrication of hydrogels," *RSC Advances*, vol. 3, no. 36, 2013.

[146] N. Pucher, A. Rosspeintner, V. Satzinger et al., "Structure –Activity relationship in d-π-a-π-d-based photoinitiators for the two-photon-induced photopolymerization process," *Macromolecules*, vol. 42, no. 17, pp. 6519–6528, 2009.

[147] X. Huang, X. Wang, and Y. Zhao, "Study on a series of water-soluble photoinitiators for fabrication of 3d hydrogels by two-photon polymerization," *Dyes and Pigments*, vol. 141, pp. 413–419, 2017.

[148] F. Terenziani, A. Painelli, C. Katan, M. Charlot, and M. Blanchard-Desce, "Charge instability in quadrupolar chromophores: symmetry breaking and solvatochromism," *Journal of the American Chemical Society*, vol. 128, no. 49, pp. 15742–15755, 2007.

[149] S. J. Bryant, C. R. Nuttelman, and K. S. Anseth, "Cytocompatibility of UV and visible light photoinitiating systems on cultured NIH/3T3 fibroblasts in vitro," *Journal of Biomaterials Science, Polymer Edition*, vol. 11, no. 5, pp. 439–457, 2000.

[150] Q. Zou, Y. Zhao, N. S. Makarov et al., "Effect of alicyclic ring size on the photophysical and photochemical properties of bis(arylidene)cycloalkanone compounds," *Physical Chemistry Chemical Physics*, vol. 14, no. 33, pp. 11743–11752, 2012.

[151] P. E. Petrochenko, J. Torgersen, P. Gruber et al., "Laser 3D printing with sub-microscale resolution of porous elastomeric scaffolds for supporting human bone stem cells," *Advanced Healthcare Materials*, vol. 4, no. 5, pp. 739–747, 2014.

[152] M. Albota, D. Beljonne, J. L. Brédas et al., "Design of organic molecules with large two-photon absorption cross sections," *Science*, vol. 281, no. 5383, pp. 1653–1656, 1998.

[153] L. Markus, O. Dmitri, J. Hilborn et al., "Two-photon degradation of a hyaluronic acid based hydrogel using a two-photon initiator as photosensitizer," *Frontiers in Bioengineering and Biotechnology*, vol. 4, 2016.

[154] L. Jonušauskas, D. Gailevičius, L. Mikoliūnaitė et al., "Optically clear and resilient free-form μ-Optics 3D-printed via ultrafast laser lithography," *Materials*, vol. 10, no. 1, p. 12, 2017.

[155] H. Ceylan, I. C. Yasa, O. Yasa, A. F. Tabak, J. Giltinan, and M. Sitti, "3D-printed biodegradable microswimmer for theranostic cargo delivery and release," *ACS Nano*, vol. 13, no. 3, pp. 3353–3362, 2019.

[156] M. Pelton, J. Aizpurua, and G. Bryant, "Metal-nanoparticle plasmonics," *Laser & Photonics Review*, vol. 2, pp. 136–159, 2008.

[157] M. Moßhammer, K. E. Brodersen, M. Kühl, and K. Koren, "Nanoparticle-and microparticle-based luminescence imaging of chemical species and temperature in aquatic systems: a review," *Microchimica Acta*, vol. 186, no. 2, p. 126, 2019.

[158] A. L. Stepanov, R. Kiyan, A. Ovsianikov et al., "Synthesis and optical properties of silver nanoparticles in ORMOCER," *Applied Physics A: Materials Science & Processing*, vol. 108, no. 2, pp. 375–378, 2012.

[159] M. J. Ventura, C. Bullen, and M. Gu, "Direct laser writing of three-dimensional photonic crystal lattices within a PbS quantum-dot-doped polymer material," *Optics Express*, vol. 15, no. 4, pp. 1817–1822, 2007.

[160] Y. Peng, S. Jradi, X. Yang et al., "3D photoluminescent nanostructures containing quantum dots fabricated by two-photon polymerization: influence of quantum dots on the spatial resolution of laser writing," *Advanced Materials Technologies*, vol. 4, no. 2, article 1800522, 2018.

[161] C. Check, R. Chartoff, and S. Chang, "Effects of nanoparticles on photopolymerization of acrylate monomers in forming nano-composites," *European Polymer Journal*, vol. 70, pp. 166–172, 2015.

[162] V. V. Rocheva, A. V. Koroleva, A. G. Savelyev et al., "High-resolution 3D photopolymerization assisted by upconversion nanoparticles for rapid prototyping applications," *Scientific Reports*, vol. 8, no. 1, p. 3663, 2018.

[163] M. Suter, L. Zhang, E. C. Siringil et al., "Superparamagnetic microrobots: fabrication by two-photon polymerization and biocompatibility," *Biomedical Microdevices*, vol. 15, no. 6, pp. 997–1003, 2013.

[164] E. Blasco, J. Müller, P. Müller et al., "Fabrication of conductive 3D gold-containing microstructures via direct laser writing," *Advanced Materials*, vol. 28, no. 18, pp. 3592–3595, 2016.

[165] J. Li, B. Jia, and M. Gu, "Engineering stop gaps of inorganic-organic polymeric 3D woodpile photonic crystals with post-thermal treatment," *Optics Express*, vol. 16, no. 24, pp. 20073–20080, 2008.

[166] D. Gailevičius, V. Padolskytė, L. Mikoliūnaitė, S. Šakirzanovas, S. Juodkazis, and M. Malinauskas, "Additive-manufacturing of 3D glass-ceramics down to nanoscale resolution," *Nanoscale Horizons*, vol. 4, no. 3, pp. 647–651, 2019.

[167] A. Vyatskikh, S. Delalande, A. Kudo, X. Zhang, C. M. Portela, and J. R. Greer, "Additive manufacturing of 3d nano-architected metals," *Nature Communications*, vol. 9, no. 1, article 593, 2018.

[168] J. K. Gansel, M. Thiel, M. S. Rill et al., "Gold helix photonic metamaterial as broadband circular polarizer," *Science*, vol. 325, no. 5947, pp. 1513–1515, 2009.

[169] F. Kotz, P. Risch, K. Arnold et al., "Fabrication of arbitrary three-dimensional suspended hollow microstructures in transparent fused silica glass," *Nature Communications*, vol. 10, no. 1, pp. 1–7, 2019.

[170] M. Boffito, F. di Meglio, P. Mozetic et al., "Surface functionalization of polyurethane scaffolds mimicking the myocardial microenvironment to support cardiac primitive cells," *PLoS One*, vol. 13, no. 7, article e0199896, 2018.

[171] M. Iqbal, D. K. Dinh, Q. Abbas, M. Imran, H. Sattar, and A. Ul Ahmad, "Controlled surface wettability by plasma polymer surface modification," *Surfaces*, vol. 2, no. 2, pp. 349–371, 2019.

[172] T. Jonavicius, S. Rekštyte, and M. Malinauskas, "Microfabrication of 3D metallic interconnects via direct laser writing and chemical metallization," *Lithuanian Journal of Physics*, vol. 54, no. 3, pp. 162–169, 2014.

[173] S. Kim, F. Qiu, S. Kim et al., "Fabrication and characterization of magnetic microrobots for three-dimensional cell culture and targeted transportation," *Advanced Materials*, vol. 25, no. 41, pp. 5863–5868, 2013.

[174] B. Dhandayuthapani, Y. Yoshida, T. Maekawa, and D. S. Kumar, "Polymeric scaffolds in tissue engineering application: a review," *International Journal of Polymer Science*, vol. 2011, Article ID 290602, 19 pages, 2011.

[175] C. D. Roskelley and M. J. Bissell, "Dynamic reciprocity revisited: a continuous, bidirectional flow of information between cells and the extracellular matrix regulates mammary epithelial cell function," *Biochemistry and Cell Biology*, vol. 73, no. 7-8, pp. 391–397, 1995.

[176] A. Folch and M. Toner, "Microengineering of cellular interactions," *Annual Review of Biomedical Engineering*, vol. 2, no. 1, pp. 227–256, 2000.

[177] J. Fink, M. Théry, A. Azioune et al., "Comparative study and improvement of current cell micro-patterning techniques," *Lab on a Chip*, vol. 7, no. 6, pp. 672–680, 2007.

[178] Y. S. Nam and T. G. Park, "Porous biodegradable polymeric scaffolds prepared by thermally induced phase separation," *Journal of Biomedical Materials Research*, vol. 47, no. 1, pp. 8–17, 1999.

[179] Y. Yang, J. Zhao, Y. Zhao, L. Wen, X. Yuan, and Y. Fan, "Formation of porous PLGA scaffolds by a combining method of thermally induced phase separation and porogen leaching," *Journal of Applied Polymer Science*, vol. 109, no. 2, pp. 1232–1241, 2008.

[180] A. Salerno, M. Oliviero, E. D. Maio, S. Iannace, and P. A. Netti, "Design of porous polymeric scaffolds by gas foaming of heterogeneous blends," *Journal of Materials Science*, vol. 20, no. 10, pp. 2043–2051, 2009.

[181] X. Wu, Y. Liu, X. Li et al., "Preparation of aligned porous gelatin scaffolds by unidirectional freeze- drying method," *Acta Biomaterialia*, vol. 6, no. 3, pp. 1167–1177, 2010.

[182] H. Yoshimoto, Y. Shin, H. Terai, and J. Vacanti, "A biodegradable nanofiber scaffold by electrospinning and its potential for bone tissue engineering," *Biomaterials*, vol. 24, no. 12, pp. 2077–2082, 2003.

[183] A.-V. Do, B. Khorsand, S. M. Geary, and A. K. Salem, "3D printing of scaffolds for tissue regeneration applications," *Advanced Healthcare Materials*, vol. 4, no. 12, pp. 1742–1762, 2015.

[184] S. Turunen, E. Käpylä, M. Lähteenmäki, L. Ylä-Outinen, S. Narkilahti, and M. Kellomäki, "Direct laser writing of microstructures for the growth guidance of human pluripotent stem cell derived neuronal cells," *Optics and Lasers in Engineering*, vol. 55, pp. 197–204, 2014.

[185] P. Danilevicius, L. Georgiadi, C. J. Pateman, F. Claeyssens, M. Chatzinikolaidou, and M. Farsari, "The effect of porosity on cell ingrowth into accurately defined, laser-made, polylactide-based 3D scaffolds," *Applied Surface Science*, vol. 336, pp. 2–10, 2015.

[186] B. Spagnolo, V. Brunetti, G. Leménager et al., "Three-dimensional cage-like microscaffolds for cell invasion studies," *Scientific Reports*, vol. 5, no. 1, article 10531, 2015.

[187] M. M. Nava, A. Piuma, M. Figliuzzi et al., "Two-photon polymerized "nichoid" substrates maintain function of pluripotent stem cells when expanded under feeder-free conditions," *Stem Cell Research & Therapy*, vol. 7, no. 1, p. 132, 2016.

[188] P. Timashev, D. Kuznetsova, A. Koroleva et al., "Novel biodegradable star-shaped polylactide scaffolds for bone regeneration fabricated by two-photon polymerization," *Nanomedicine*, vol. 11, no. 9, pp. 1041–1053, 2016.

[189] A. Marino, C. Filippeschi, G. G. Genchi, V. Mattoli, B. Mazzolai, and G. Ciofani, "The osteoprint: a bioinspired two-photon polymerized 3-D structure for the enhancement of bone-like cell differentiation," *Acta Biomaterialia*, vol. 10, no. 10, pp. 4304–4313, 2014.

[190] E. E. Morales-Delgado, L. Urio, D. B. Conkey, N. Stasio, D. Psaltis, and C. Moser, "Three-dimensional microfabrication through a multimode optical fiber," *Optics Express*, vol. 25, no. 6, pp. 7031–7045, 2017.

[191] R. Whitby, Y. Ben-Tal, R. MacMillan et al., "Photoinitiators for two-photon polymerisation: effect of branching and viscosity on polymerisation thresholds," *RSC Advances*, vol. 7, no. 22, pp. 13232–13239, 2017.

[192] K. Obata, S. Slobin, A. Schonewille et al., "UV laser direct writing of 2D/3D structures using photo-curable polydimethylsiloxane (PDMS)," *Applied Physics A*, vol. 123, no. 7, p. 495, 2017.

[193] A. Q. Liu, W. M. Zhu, D. P. Tsai, and N. I. Zheludev, "Micromachined tunable metamaterials: a review," *Journal of Optics*, vol. 14, no. 11, article 114009, 2012.

[194] T. Bückmann, N. Stenger, M. Kadic et al., "Tailored 3D mechanical metamaterials made by dip-in direct-laser-writing optical lithography," *Advanced Materials*, vol. 24, no. 20, pp. 2710–2714, 2012.

[195] J. Qu, A. Gerber, F. Mayer, M. Kadic, and M. Wegener, "Experiments on metamaterials with negative effective static compressibility," *Physical Review X*, vol. 7, no. 4, article 04106, 2017.

[196] B. Stępak, A. J. Antończak, M. Bartkowiak-Jowsa, J. Filipiak, C. Pezowicz, and K. M. Abramski, "Fabrication of a polymer-based biodegradable stent using a CO_2 laser," *Archives of Civil and Mechanical Engineering*, vol. 14, no. 2, pp. 317–326, 2014.

[197] S. Rekštyte, D. Paipulas, M. Malinauskas, and V. Mizeikis, "Microactuation and sensing using reversible deformations of laser-written polymeric structures," *Nanotechnology*, vol. 28, no. 12, article 124001, 2017.

[198] L. Jonušauskas, S. Rekštyte, and M. Malinauskas, "Augmentation of direct laser writing fabrication throughput for three-dimensional structures by varying focusing conditions," *Optical Engineering*, vol. 53, no. 12, article 125102, 2014.

[199] F. Mayer, S. Richter, J. Westhauser, E. Blasco, C. Barner-Kowollik, and M. Wegener, "Multimaterial 3D laser microprinting using an integrated microfluidic system," *Science Advances*, vol. 5, no. 2, article eaau9160, 2019.

[200] D. Gräfe, A. Wickberg, M. M. Zieger, M. Wegener, E. Blasco, and C. Barner-Kowollik, "Adding chemically selective subtraction to multi-material 3D additive manufacturing," *Nature Communications*, vol. 9, no. 1, p. 2788, 2018.

[201] K. Obata, J. Koch, U. Hinze, and B. N. Chichkov, "Multifocus two-photon polymerization technique based on individually controlled phase modulation," *Optics Express*, vol. 18, no. 16, pp. 17193–17200, 2010.

[202] D. Yang, L. Liu, Q. Gong, and Y. Li, "Rapid Two-Photon Polymerization of an Arbitrary 3D Microstructure with 3D Focal Field Engineering," *Macromolecular Rapid Communications*, vol. 40, no. 8, article 1900041, 2019.

[203] C. F. Phelan, R. J. Winfield, D. P. O'Dwyer, Y. P. Rakovich, J. F. Donegan, and J. G. Lunney, "Two-photon polymerisation of novel shapes using a conically diffracted femtosecond laser beam," *Optics Communication*, vol. 284, no. 14, pp. 3571–3574, 2011.

[204] E. Stankevicius, T. Gertus, M. Rutkauskas et al., "Fabrication of micro-tube arrays in photopolymer SZ2080 by using three different methods of a direct laser polymerization technique," *Journal of Micromechanics and Microengineering*, vol. 22, no. 6, article 065022, 2012.

[205] R. D. Loor, "Polygon scanner system for ultra short pulsed laser micro-machining applications," *Physics Procedia*, vol. 41, pp. 544–551, 2013.

[206] G. R. B. E. Romer and P. Bechtold, "Electro-optic and acousto-optic laser beam scanners," *Physics Procedia*, vol. 56, pp. 29–39, 2014.